The Impact of CD40L on Mature Dendritic Cell and Their EV Production

by

Joseph Michael McNulty

Bachelor of Science in Biology, John Carroll University, 2021

Submitted to the Graduate Faculty of the

School of Public Health in partial fulfillment

of the requirements for the degree of

Master of Science

University of Pittsburgh

2023

UNIVERSITY OF PITTSBURGH

SCHOOL OF PUBLIC HEALTH

This thesis was presented

by

Joseph Michael McNulty

It was defended on

April 20, 2023

and approved by

Joshua Mattila PhD
Assistant Professor
Infectious Diseases and Microbiology
School of Public Health
University of Pittsburgh

Adrian Morelli MD, PhD
Professor of Surgery and Immunology
T.E. Starzl Transplantation Institute
University of Pittsburgh

Thesis Advisor:
Robbie Mailliard PhD
Visiting Associate Professor
Department of Medicine, Division of Infectious Diseases
University of Pittsburgh

The Impact of CD40L on Mature Dendritic Cell and Their EV Production

Joseph Michael McNulty, MS

University of Pittsburgh, 2023

As HIV becomes a more chronic and manageable condition, research of the disease has shifted. ART has played a large role in raising the life expectancy of people living with HIV. However, it has some drawbacks and has created a landscape for the need of a novel and more effective therapeutic to eradicate HIV. The dendritic cell (DC) shows promise as a role player in this novel therapeutic due to its ability to link both the innate and adaptive arm of the immune systems. Several studies have shown that type-1 polarized DCs (DC1s) are more effective at driving latency reversal and CTL responses, when stimulated with CD40L, a costimulatory molecule derived from CD4+ T helper cells that has many immunologic functions. A clinically relevant type-1 polarized DC vaccine platform called the alpha-DC1 (αDC1) developed at the University of Pittsburgh is currently being studied as an alternative to more commonly used DC-based vaccines, sometimes referred to as DC2. To accurately compare the two DC subsets and to gain a better understanding of each cell type and their interaction with other immune cells, we performed tests to detail the characterization of these DC-based vaccine platforms and their responsiveness to the T helper cell signal CD40L. We assess their differences through characterization of their phenotype, morphology, cytokine production, single cell transcriptomics, and extracellular vesicle production. It is understood that the knowledge obtained from this study would give researchers an in-depth understanding of these clinically relevant DC subsets so that they may be used more effectively as an HIV therapeutic.

Table of Contents

List of Figures

Preface

I would first like to thank my advisor Dr. Robbie Mailliard for all of the help and guidance throughout my master's degree. Through his mentorship I was able to grow and mature not only as a scientist and a student but as a person as well. The experiences I will take from this program and Dr. Mailliard are assuredly ones that I will use for the rest of my life, and I am eternally grateful for those. I would like to thank my lab members, Holly Bilben, Peter Shoucair, Sube Govinda Rajan Ravi, Grace Bothwell, Lexi Mullen, and especially Ally Depuyt for all of the help, guidance and friendship during my time in the Mailliard Lab. I also would like to thank Pittsburgh Fitness Project and Tom Duer for being a mentor figure outside of the lab and helping me find a home after moving to a new state when I came to Pittsburgh. Lastly but certainly not least, I would like to thank my mother and father, Diana and Michael, and my younger brother Sam for always supporting my goals, dreams, and ambitions. I am who I am today because of all of you.

1.0 Introduction

According to the W.H.O., in 2019 there were 36.8 million people living with HIV, with 1.99 million new infections, and 863,867 deaths from HIV. Thirty years ago, the idea that human immunodeficiency virus (HIV) infection could be a manageable chronic condition would have been incomprehensible. Since the advent of antiretroviral therapy in 1991, the scope of how HIV infection is viewed has changed. This has caused a drastic increase in the life expectancy of people living with HIV, it is now near that of the general population. [1] Antiretroviral therapy (ART) has been incredibly effective in protecting those infected with HIV and preventing the further spread of HIV. However, he usage of ART has created some challenges Many of these therapy regimens require strict adherence, and their effectiveness is limited in certain tissue sites; Moreover, there are always concerns for the development of resistance to the drugs.[2] ART works suppressing the viral load of an individual but does not clear the infection entirely. When an individual stops ART, the latent HIV reservoir reactivates, and their viral load rapidly increases. Because of this, there is a push to investigate different mechanisms that would allow for either the elimination of HIV entirely or a functional cure through immunologic means.

One of these therapeutic concepts in development is known as the “kick and kill” approach. The approach involves implementing a latency reversal agent (LRA) as “the kick” to induce the activation of the latent proviral DNA latently in infected cells. This would promote production of antigenic targets for immune effector cells, such as HIV specific cytotoxic T lymphocytes (CTLs), to recognize and “kill” the infected cells [3]. There are several different categories of LRAs, among them are epigenetic modifiers such as histone deacetylase inhibitors (HDACi), methyl transferase inhibitors, methylation inhibitors and bromodomain inhibitors), protein kinase C agonists,

activators of the PI3K pathway including disulfiram and mTOR inhibitors), and NFkB agonists. [4] While these LRAs have been shown to increase viral RNA expression, it is unclear whether their reversal is effective enough to drive antigen specific elimination of the reservoir. [5] Along with that, some studies have shown that certain LRAs have a toxic effect on CTLs, which would be counterproductive for a kick and kill mechanism of HIV control. [6]

Some areas of research have gone into looking at engineered nanoparticles (particles 1-100nm) as an effective method of enhancing LRA delivery. Originally nanoparticles have been used to improve antiretroviral therapy by increasing the rigidity of delivery time. The nanoparticles achieve this by utilizing a 'long-acting slow-effective' release antiretroviral therapy [7] This focus of nanoparticles has rapidly expanded with the growing field of extracellular vesicle (EV) research. The intercommunication that EVs mediate between cells has been targeted as a possible mechanism for therapeutic focus. [8] In a 2017 publication by Zaccard et.al, it was shown that monocyte derived αDC1s create F-actin tunnelling nanotube structures (TNTs) when stimulated with CD40L, a molecule that is expressed on CD4+ T cells. [10] The TNTs were observed aiding in the direct transfer endogenous and exogenous material from cell to cell. One mechanism in which the transfer was also found to occur was through what appeared to be the release of EVs from these TNT structures. (Zaccard et al,, unpublished) Then a recent publication by Kristoff et.al which showed that αDC1s loaded with HIV and CMV antigen could drive both the "kick" and the "kill" , by driving latency reversal while simultaneously driving a targeted CTL response against the infected CD4+ T cells. [9] This gives rise to the idea that monocyte derived αDC1s and the extracellular vesicles they produce could play a complementary role in forming novel therapeutic strategies for the elimination or control of the latent HIV reservoir.

1.1 The Dendritic Cell

1.1.1 Discovery

The discovery of the dendritic cell was a result of researching deeper into understanding the mononuclear phagocyte system, which had been known to play roles in adhering to, engulfing, and degrading pathogens. However, the role of driving an immunological response was not yet fully understood. In 1960, it was shown that glass-adherent mouse cells from the spleen could drive an adaptive immune response. This led to the speculation of a possible antigen-presenting cell, a type of cell that could take up antigen and partially degrade it so that it could be presented on the cell surface as a means to stimulate other cell types. This was not confirmed until 1973 when scientist Ralph Steinman who was working as a post-doctoral fellow in the laboratory of Zan Cohn at Rockefeller University, discovered a small population of cells with unique stellate morphology during microscopic study of the glass-adhering mouse splenocytes, and named them dendritic cells based on the dendrite like protrusions that he saw, reminding him of neurologic dendrites. [11 Further studies highlighted their superior antigen presenting ability, characterized by their remarkable ability to efficiently take up and process extracellular antigen for subsequent surface presentation in the context of MHC-1 and MHC-II complexes as a means to prime and educate naïve T cells within lymphoid tissues. [12] This cross-presentation capacity along with their ability to respond to and interpret danger signals they receive in the peripheral tissues allows them to act as the bridge of the immune system, as they directly link the innate and adaptive arms.

1.1.2 Immunological Function

There are different DC subsets, each having distinct functions. DCs form within the bone marrow and arise from lympho-myeloid hematopoiesis. [13] They play a role in both arms of the immune system as they interact with pathogen associated molecular patterns (PAMPs) as immature DCs (iDCs). They survey and take up antigen. Together, this causes them to mature and thus express the antigen on their surface through an MHC complex. These mature DCs are able to prime naïve T cells and stimulate the adaptive immune response after migrating to the lymph node. This is the immune function that makes them not only critical to successfully clearing a pathogen, but also a prime target for any therapeutic or vaccine. [14] Maturation of iDCs happens through not only pathogen associated factors, but indirectly through interactions with other cytokines and chemokines produced during infection. The different combination of maturation factors leads to the different functional subsets of DCs, each having distinct functional qualities.

Figure 1: Ontological overview and functional specialization of human dendritic cells

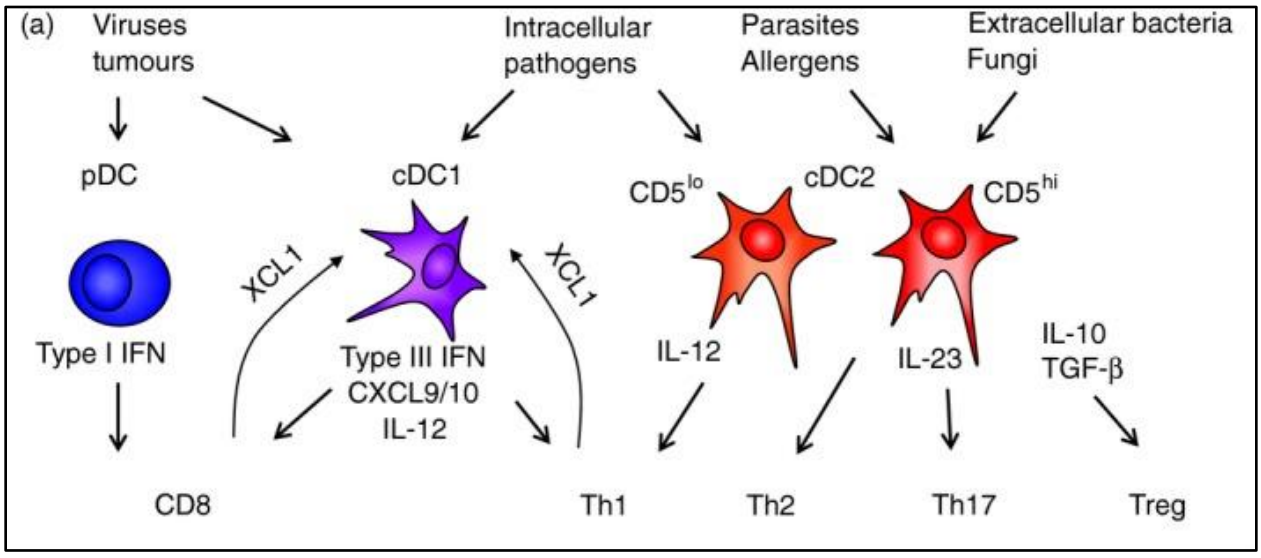

(A) DC are often depicted as a single 'all purpose' cell in diagrams of T-cell differentiation but each subset is specialized to make specific responses to pathogen or danger signals. Depending on the context, many different responses may be observed and selected principal functions of human plasmacytoid DC (pDC), conventional DC1 (cDC1) and cDC2 are depicted. [13]

1.1.3 Dendritic Cells and Driving Specific Immune Responses

As previously mentioned, there are different classes of naturally occurring DCs and each of them have their unique function. Conventional dendritic cells (cDCs) can be broken down into two different categories, cDC1, and cDC2s. Both are powerful APCs; however, they present antigen differently from one another. cDC1s present cell-surface antigen through MHC-I and stimulate a CD8+ T cells, driving supporting Th1 responses through their production of IL-12p70. cDC2s tend to drive a stronger Th2 response by activating CD4+ T cells through the MHC-II in the absence of IL12p70. Plasmacytoid DCs are not considered to be good APCs but are superior at producing antiviral type-1 interferons. [15] Complex interactions between the DC and the T cell occurs through several critical cell surface molecules. One of those are the MHC complex binding to the TCR, which is sometimes referred to as Signal 1. The second of those molecules is

a costimulatory molecule of either CD80 or CD86 binding to CD28 on the T cell. This binding is critical for full activation of the T cell, without it the T cell goes through anergy. This is known as Signal 2. [16] The DCs release different cytokines and stimulatory molecules that drive the differentiation of the naïve T lymphocyte. Referred to as Signal 3, this plays a critical role in determining the differentiation of the T cell into its specific effector cell type and the cytokines it is capable of producing. This is where the diversity of the DC shines in its ability to regulate the immune system based on the different cytokines it produces. [17]

1.2 CD40L

1.2.1 Molecular Structure

CD40L, also known as CD154 and TNFSF5, is a type II membrane glycoprotein and one of the members of the tumor necrosis factor (TNF) superfamily of molecules. It contains a 22 amino acid cytoplasmic tail, a 24 amino acid transmembrane domain and a 215 amino acid extracellular domain. It is assembled by the cell in sever different forms. Among those are noncovalent homotrimers and as heterotrimers existing in both a truncated and nontruncated form of the molecule. It binds to CD40 which is found on several different APCs and it has a large variety of functions as it is found biologically in both a soluble form and a membrane form. [18]

1.2.2 CD40/CD40L Interaction

Outside of the Signal 2 costimulatory function of the CD80 and CD86 (B7 family**)**/CD28 interactions there is another main driver of Signal 2 and that is the TNFR family. The CD40/CD40L interaction is one of the larger interactions along with OX40/OX40L interactions that is seen in the TNFR family. This interaction helps to drive activation of T cells just like the B7 family/CD28 interaction does. Along with T cell activation and differentiation, the CD40/CD40L interaction causes an increase in cytokine production, promotes germinal center formation, isotype switching, and promotes cellular longevity. [19] CD40 is not just expressed on DCs, it is also expressed on B cells, monocytes and hematopoietic cells. Because of this diversity, the CD40/CD40L interaction plays a role in both humoral and cell mediated immunity. [20]

1.2.3 CD40L as a Novel Helper Factor in Driving a CTL Response

A commonly understood interaction is the role of CD4+ T helper cells in driving a robust CTL response. Much of this help occurs through signaling of the CD40 molecule on the DC. It has been shown that stimulation of the CD40 molecule allowed for the priming CD8+ CTL responses without the need of CD4+ T cell help. This showed that the CD40-CD40L, expressed on CD4+ T helper cells, plays a role in cross-talk with the DC to create a CTL response, something that is beneficial in a kick and kill mechanism of therapeutic. [21] CD40L drives the production of IL-12p70 in stimulated DCs, which is thought to be the driving cytokine in a robust Th1 response leading to effective priming and CTL response. [22]

What is important to note about this CD40-CD40L interaction is that the different subsets of DC react differently to stimulation of CD40. Monocyte derived DC2, which are generated *in*

vitro in the presence of prostaglandan-2 (PGE-2) produce much higher levels of IL-12p40, which is actually an inhibitor of IL-12p70. IL-12p70 is comprised of IL-12p40 and IL-12p35. Without IL-12p35, the molecule is biologically inactive and does not play any proinflammatory role. [22] It can be seen as well that αDC1s produce much larger amounts of IL-12p70 than that of their DC2 counterparts. [10] This then points back to the viability of αDC1s as a prime candidate of the "kill" aspect of the "kick and kill" therapeutic concept.

Along with differences in IL-12p70 production, CD40L has been shown to induce long tunneling nanotube formations in αDC1s in comparison to the DC2s. This is an example of CD40L driving the hyper-activation of the αDC1s. [10] The role of CD40L in immunoregulation has also been demonstrated in the upregulation of PDL-1 surface expression on the αDC1s. [23] This is particularly interesting because typically PDL-1 is a CTL inhibitor in when it binds to PD-1 on activated CTLs, but in the context of DCs, it has also been noted as supportive to naïve T cell differentiation, which is completely different to its interaction with effector T cells. [23]

1.3 Extracellular Vesicles

1.3.1 Discovery of EVs

Extracellular vesicles are relatively new to the research world. Having only entered the topic of biologic relevance during the 80s and 90s, there is still much to learn. Despite the topic of EV becoming well known, previous research from years before had pointed to their existence, even before we could see them. The advent of EVs came from the work of Erwin Chargaff, a chemist, and Randolph West, a clinician. The two of them were investigating the coagulation of

blood and what they noticed was that while creating a protocol to isolate clotting factors from cells they saw “the addition of the high-speed sediment to the supernatant plasma brought about a very considerable shortening of the clotting time.” What they had isolated would later go on to be identified as extracellular vesicles. This was in 1946, some 35 years before the field of EV biology began to take off. [24] With the first usage of the term multivesicular body in 1974, the field began to expand in during the 80’s there was a rapid expansion into the field of EVs. It would still be another twenty or so years before the field began to develop any uniformity in thought [24] Much of the previous work was done on platelets, but a publication in 1996 caught the eye of many different researchers. Raposo et.al showed that B lymphocytes could secrete vesicles that contained antigen and more importantly, that these vesicles could present antigen to another cell through MHC-II that was present on the vesicle. [25] From the late 90’s to current the field has started to solidify nomenclature, developed field specific journals and societies, and have aided in the rapid expansion of the field. With that being said, the field is still rapidly expanding and there is still so much information left to learn about EVs and their biological functions.

1.3.2 EV Formation and Nomenclature

EVs are lipid bound vesicle structs that carry various different types of cargo from proteins to antigen, to mRNA, to miRNA, and various metabolites. [27] Extracellular vesicles currently are separated into three different categories. These categories are based on both size and mode of formation. The smallest of the group are exosomes or small extracellular vesicles. Exosomes are formed in three different stages. The first stage is the invagination of the plasma membrane which creates endocytic vesicles. These endocytic vesicles then go through a process of inward budding of the membrane to create a multivesicular body (MVB). This MVB then fuses with the cell

membrane and releases the exosomes into the extracellular environment. Exosomes typically have a size range of less than 150nm. Exosomes have a complex relationship with several different intracellular proteins, which all play large roles in their formation. These proteins being endosomal complexes required for transport (ESCRT) proteins, GTPases, Rab proteins, apoptosis-linked gene 2-interacting protein X (ALIX), syndecan-1, phospholipids, tetraspanins, ceramides, sphingomyelinases, and SNARE [soluble N-ethylmaleimide-sensitive factor (NSF) attachment protein receptor] complex proteins. [29] The distinct interaction that these proteins have with one another still has yet to be fully elucidated, but the process of exosome formation is known to be complex and depends on many contributing factors.

Microvesicles are the second category of EVs, they range in size from 100-1000nm in size. Microvesicles form from the outward budding of the cell membrane, therefore they carry more material directly related to the cell membrane in comparison to the exosomes. [28]

The final group of EVs are apoptotic bodies, sometimes also referred to as necrotic bodies. They form when the cell goes through apoptosis and the cell membrane buds off while still holding onto some intracellular material. These have the largest size of greater than 1000nm. [29] The majority of the relevant research is focused upon exosomes due to their complex formation and ability to carry intracellular information. Because there can be overlap in size and origin cannot always be validated, much of the labeling has transitioned into using the term EV to attempt to eliminate as much confusion as possible. [26]

1.3.3 Characterization of EVs

There are different ways to analyze and characterize EVs, and this can be done to assess size, purity, membrane proteins, and internal cargo. Imaging of EVs is typically performed using

an electron microscope. EVs are seen as grey blobs that are around 100nm in size, give or take. [30] Size can also be determined through nanoparticle tracking analysis, or NTA. NTA uses Brownian motion and the Stokes-Einstein equation to deduce the size of the EVs in the samples and the concentration of the sample. It is a better method to use than dynamic light scattering due to NTA's ability to analyze heterogeneous populations whereas DLS tends to favor the larger nanoparticles as the light scattering off them skews the other data points. [28] Protein analysis can be done several different ways. The most common way is through western blotting. Several distinct molecules are seen with high frequency in EVs, so they make good markers to help identify the product as containing EVs. The molecules are CD63, CD9, and CD81 which are members of the tetraspanin family and are expressed on the membrane of the EVs. Another good marker especially for western blotting is TSG101 which is a protein often found internally as it plays a role in EV formation. [28] Internal cargo can be assessed in a number of ways such as through microarrays, bulk RNA sequencing, and targeted proteomics such as mass spectroscopy. Each of these techniques has their benefits and their drawbacks. For instance, microarrays must use already known markers therefore, a whole population of miRNA may be missing. Bulk RNA sequencing may run into issues with low input volumes causing skewed or poor-quality data. Similar to microarrays, mass spectroscopy requires an already known set of proteins to target during the analysis process.

Figure 2: Hallmarks of exosomes

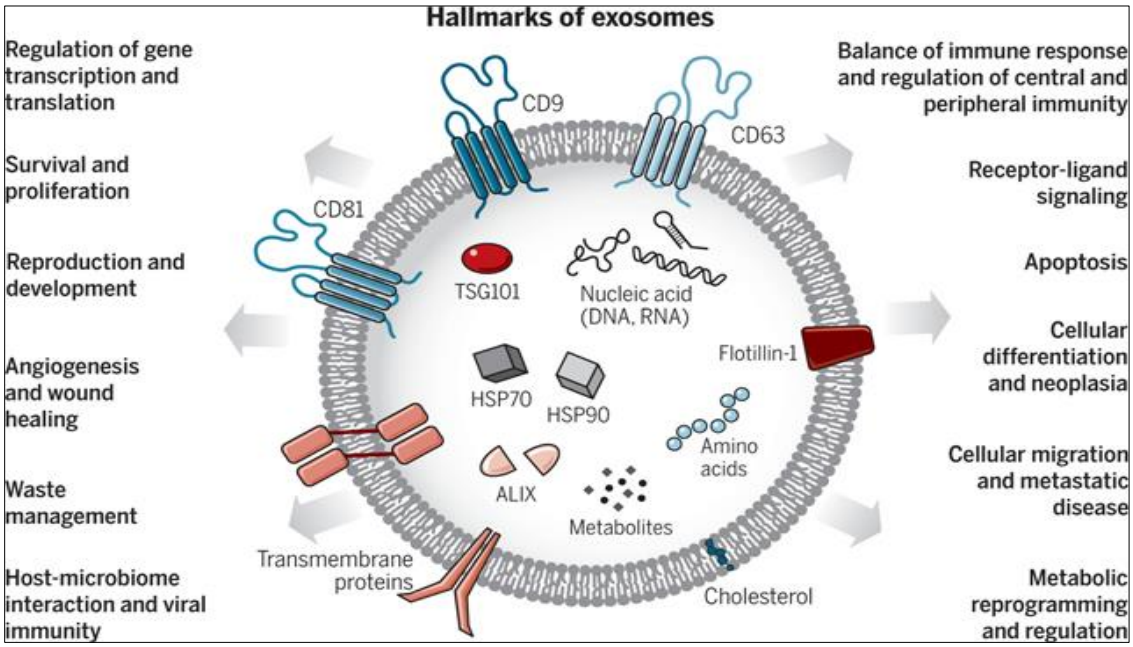

Figure to the right displays the vast number of functions that exosomes play a role in. [29]

2.0 Overarching Project Goal

Pulling from the background information and the scientific rationale that was displayed, I hypothesize that there are distinct differences between αDC1s and DC2s when stimulated with CD40L that have not yet been compared between the subsets. Furthermore, I hypothesize that when the differentially polarized DCs interact with CD40L, they create extracellular vesicles that are distinctly different from one another, and these EVs can play a role in intracellular communication. This hypothesis is based on the premise that αDC1 undergo unique physical changes upon interaction with CD40L during the process of reticulation where they form tunneling nanotubes that could act as a vessel for the release of EVs into the extracellular environment. Moreover, previous studies from the Storkus group described the transfer of T-bet from adoptively transferred DC1 to recipient T-bet deficient T cells *in vivo* in a T-bet deficient mouse model. This occurred through some unknown mechanism and was speculated to be through EV delivery. It is my position that DC1 production of EVs has a wide range of immunologic functions, including the delivery of co-stimulatory molecules, cytokines, and transcription factors that together can contribute to T cell priming and directed education as part of the DC mediated "Signal 3". For my thesis, the overarching goals were 1.) to perform deep characterization of the two clinically relevant DC subsets (αDC1 and DC2) with and without stimulation from CD40L and 2.) establish a protocol for the isolation and characterization of DC-derived EVs and assess the differences between EVs isolated from αDC1 and DC2 with and without stimulation of CD40L.

Successfully addressing the aims stated will allow for a more in-depth understanding of the role CD40L plays in creating an effective DC-based and DC EV-based therapeutic strategies to treat chronic diseases including cancer and HIV infection. . By understanding the role that

CD40L plays in formation of EVs gives greater insight to the role that DC-derived EVs play in immune signaling between T cells and DCs.

3.0 Specific Aims

3.1 Aim 1: Deep Characterization of the Differently Matured Dendritic Cells (αDC1, and DC2)

The focus of this aim is to develop an in depth understanding of the differences and similarities between the two DC subsets and compare them with and without stimulation from CD40L. We hypothesize that the αDC1 when stimulated with CD40L will be the most biologically active of the subsets, becoming the most polarized and highest producing population of cells. We will test this hypothesis through the following subaims:

1. Characterize the phenotype, morphology, and function of differentially polarized DCs during their resting state and following CD40L stimulation
2. Perform transcriptomic analysis of the differentially polarized DC with and without CD40L stimulation.

3.2 Aim 2: The Isolation and Characterization of DC-Derived EVs from Differentially Polarized Dendritic Cells (αDC1, and DC2)

The focus of this aim is the development of a protocol for the isolation of EVs from DCs in the Mailliard lab and assess the effect that CD40L stimulation of the parent cell has on the phenotypic and functional characteristics of the EVs. We hypothesize that CD40L will cause an increase in EV production, that the αDC1s will produce the most EVs out of the different

conditions, and that the EVs produced when stimulated with CD40L will carry different vesicular cargo in comparison to the unstimulated condition, and the cargo of the EVs will greatly depend on the mode of DC maturation. We will test these hypotheses through the following subaims:

1. Establish a laboratory protocol for the successful generation and isolation of extracellular vesicles from DCs.
2. Characterize DC-derived EVs generated during DC resting state and following CD40L stimulation both phenotypically and morphologically
3. Conduct transcriptomic analysis of DC-derived EVs generated during resting state and following CD40L stimulation

4.0 Materials and Methods

4.1 Isolation of Primary Cells from Blood

Peripheral blood mononuclear cells (PBMCs) were isolated from whole blood products from the Pittsburgh Blood Bank and from the participants of the Multicenter AIDS Cohort Study (MACS). The PBMCs were isolated using a density gradient separation technique that uses lymphocyte separation medium from Corning (Cat# 25-072-CV). Once the gradient containing the PBMCs was isolated, the cellular contents were separated further into monocytes and peripheral blood lymphocytes (PBLs). This was done using a CD14+ immunomagnetic negative selection method by Easysep: STEMCELL Technologies Inc., Vancouver, BC, Canada.

4.2 Generation of Human Monocyte Derived Dendritic Cells

The generation of monocyte derived dendritic cells for cellular analysis started first with the plating of monocytes on a 24 well Ultra-Low Binding Plate (Corning, TCA-3473). Cells are plated at a concentration of 500,000 – 800,000 monocytes/mL. Monocytes were cultured in IMDM containing 10% FBS (Gibco, Life Technologies, Grand Island, NY) and stimulated for 5 days with Graulocyte-macrophage colony-stimulating factor (GM-CSF) and Interleukin 4 (IL-4) both at a concentration of 1000 IU/mL (R&D Systems, Minneapolis, MN) to create immature Dendritic cells (iDCs). These iDCs are then stimulated for 48hr with different cytokine cocktails to induce differential polarization. iDCs set to polarize into αDC1s are stimulated with TNF-α (50 ng/mL),

IL-1β (25 ng/mL), IFN-α (3000 units/mL), IFN-γ (1000 units/mL) and polyisosinic: polycytidilic acid (Poly I:C) (20 ug/mL). iDCs set to mature and polarize into DC2s consisting of IL-6 (1000 units/mL), PGE2 (10^{-6} mol/L), IL-1β and TNF-α. Mature dendritic cells were then harvested washed 3 times in RPMI, and ready for use.

4.3 Stimulation of Dendritic Cells with CD40L

Matured DC subsets were plated at 25,000 cells per well / 200ul of AIM V media in a 96 well flat-bottom plate and treated with three conditions: unstimulated, stimulated by CD40L-J558 cells (Mouse Plasma cell myeloma cell line that has a transfected gene for the production of CD40L) and stimulated by rhCD40L (MegaCD40L, Enzo Life Sciences). DCs were cocultured with CD40L-J558 cells at a 1:2 ratio of DCs to J558s. Cells stimulated with rhCD40L were stimulated with 5ug/mL. After 24hrs post stimulation, the supernatants were collected and stored in a -80°C freezer until usage.

4.4 Light Microscopy of DCs

αDC1s and DC2s were observed and imaged on day 7 of stimulation, under an inverted standard light microscope to assess for morphologic differences between the subsets of DCs. Images were taken using a Leica DM IL LED Inverted Laboratory Microscope. Images were taken at 200x magnification and were taken using the LAS X Imaging Software.

4.5 Flow Cytometry Analysis of DCs

Cells collected on day seven from each of the different mature DC subsets and plated at 25,000 cells/well. Cell surface staining of the DCs was carried out by first pelleting cells by centrifugation and incubating the disrupted cell pellet with the fluorescent antibodies for 15 mins. The stains used were CD83 PE (Beckman Coulter, cat # PNIM2218), CD86 PE (Beckman Coulter, cat # IM2729), CCR7, Anti -hccR7 Fitc (R&D, Fab197F), Siglec1 (Biolegend,PE antihuman CD169 sialadhesin, siglet 1 clone 7-239 mouse IgG1 Cat # 3460), OX40L (BD Pharmigen, PE Mouse anti human ligand Cat # 558164). Samples were then washed in PBS containing 0.1% sodium azide, fixed in 1% PFA and data were collected on the BD LSR Fortessa Cell Analyzer with BD FACSdiva software. Data analysis was conducted using BD's FlowJo analysis software.

4.6 Cytokine Production Analysis

The supernatants from the differentially polarized and CD40L stimulated DC cultures were analyzes for cytokine content using the Meso Scale Discovery (MSD) multiplex system. MSD multiplex kits were used to sample a broad array of cytokines produced from the differentially polarized DCs. The two MSD kits used were the U-PLEX Macrophage M1 Combo 1 (human) cat. (K15336K), for detections of the following cytokines: IL-1β, IL-6, IL-18, Il-23, IL-12p70, IP-10, MCP-1, MIP-1α, and TNF- α; and the U-PLEX Macrophage M2 Combo 1 (human) cat. (K15337K), which was used to detect the following cytokines: Eotaxin-2, IL-4, IL-10, IL-13, M-CSF, MDC, TARC. The MSD plate was read on the MESO SECTOR S 600MM

Ultra-Sensitive Plate Imager and analyzed using the Discovery Workbench 4.0 Analysis software. Data were then exported and imported into GraphPad Prism 9 for further graphical analysis.

4.7 Single Cell Sequencing

Single cell sequencing was conducted using the BD Rhapsody system. DCs were cultured based upon the previously described methods and harvested on day 7 of the culture. The DCs were then replated and stimulated was CD40L for a period of 4 hours at 5% CO_2 and 37°C before being harvested for single cell analysis. The four conditions used were αDC1, αDC1+CD40L, DC2, DC2+CD40L. The samples were multiplexed following BD's single cell sequencing protocol and 54,000 cells were loaded onto the cartridge that has a max cell count of 40,000 cells. After the capture period the machine read the number of cells on the cartridge as about 39,000 cells. From there the cells were tagged with the beads for single cell analysis and that came back with a total of 25,000 bead-cell combinations for sequencing, which is about 6,250 cells per condition to be sequenced. The library prep was prepared following BD's single cell sequencing protocol and the samples were checked for purity using an Agilent TapeStation located at the Single Cell Genomics Core at the University of Pittsburgh. Samples were then sent to the Emory Integrated Genomics Core located in the Emory University School of Medicine. Data from NGS was uploaded onto Seven Bridges Genomics where it went through basic quality screening. Data were then pulled from Seven Bridges Genomics where it was analyzed using a bioinformatics R-based single-cell analysis software by a PhD candidate who was partnering on the project, Ally Depuyt.

4.8 Generation of Monocyte Derived DCs for Extracellular Vesicle Isolation

The generation of monocyte derived DCs for EV isolation started first with the plating of monocytes on a 24 well Ultra-Low Binding Plate (Corning, TCA-3473). Cells are plated at a concentration of 800,000-10^6 monocytes/mL. Monocytes were cultured in AIM-V, a serum free media (Gibco, Life Technologies, Grand Island, NY) and stimulated for 4 days with GM-CSF and IL-4 both at a concentration of 1000 IU/mL (R&D Systems, Minneapolis, MN) to create immature DCs (iDCs). These iDCs were differentially matured and stimulated with CD40L as described earlier.

4.9 Extracellular Vesicle Isolation

Cell culture media is taken and centrifuged at 1600 rpm for 10 minutes to pellet out the cells. The supernatant is taken from that sample and centrifuged at 10,000 x g for 30 minutes at 4-8°C to pellet out all of the microvesicles using a Sorvall RC-3C+ Refrigerated Centrifuge. Samples are then removed from the centrifuge tube and concentrated down to 500uL of sample using Cytiva Vivaspin™ 6 Sample Concentrators (cat. 45-001-576). These concentrators have a molecular weight cutoff of 100,000. The concentrated sample is then isolated via size using a size exclusion chromatography method. Following the protocol for IZON's qEVoriginal / 35nm Legacy Column, 16 fractions were taken and the EV containing fractions were pooled together for further analysis. The Cytiva Vivaspin™ 6 Sample Concentrators were used to concentrate the pooled sample if needed for specific analysis methods.

4.10 Verification of EV Fractions via Nanodrop

16 EV fractions were taken at a volume of 500uL per fraction. The protein in each sample was quantified using the NanoDrop Microvolume Spectrophotometer using an absorbance of A280 and quantified in ug/mL. According to IZONs protocol, the first three fractions displaying a spike in protein will be the fractions containing the EVs. Once those were identified the samples were pooled for further analysis.

4.11 Size Quantification of EVs

10uL of each EV sample was taken for analysis of size and concentration using nanoparticle tracking analysis. Each sample was diluted to a 1:500 dilution and analyzed using The Malvern Panalytical NanoSight LM10. A total of three videos were taken for each sample and the data were analyzed using the Nanoparticle Tracking Analysis Software also by Malvern Panalytical.

4.12 Bead Based Flow Cytometry Analysis of EVs

Isolated extracellular vesicle samples were concentrated down to 200uL of sample by using the Cytiva Vivaspin™ 6 Sample Concentrators. Using the Exosome – Human CD63 Isolation/Detection From Cell Culture Media dynabeads (Invitrogen, Life Sciences, cat#10606D), extracellular vesicles were bound to the beads using an overnight incubation in a cold room on a

rocker. After washing, the bead bound exosomes were incubated with fluorescent antibodies for one hour. The antibodies used were CD63 PE (BD Pharmingen, cat# 561925), CD9 PE (BD Pharmingen, cat# 555372), CD81 PE (BD Pharmingen, cat# 566714). The beads are then washed and fixed with PFA. Samples were then ran on the BD LSR Fortessa Cell Analyzer and data were collected using the BD FACSdiva software. Data analysis was conducted using BD's FlowJo analysis software.

5.0 Results

5.1 Aim 1: Deep Characterization of the Differently Matured Dendritic Cells (DC1 and DC2)

5.1.1 Morphologic Characterization of Differentially Polarized DC

Figure 3: Light microscopy of differentially polarized dendritic cell types

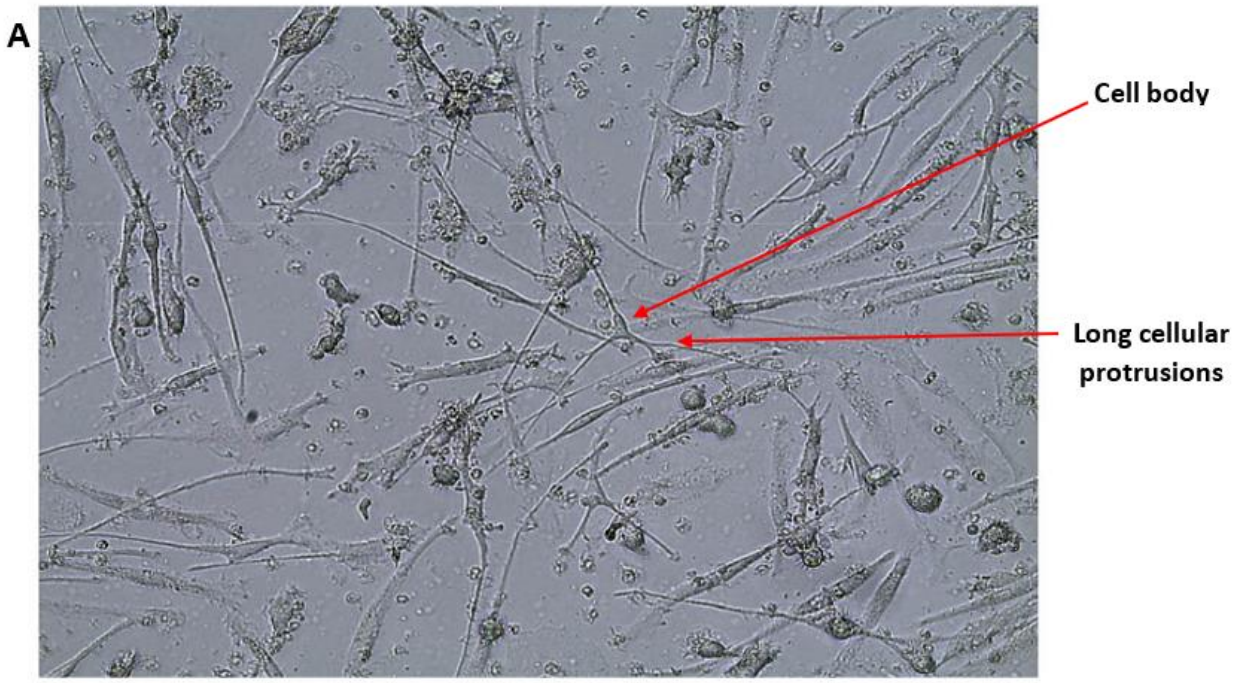

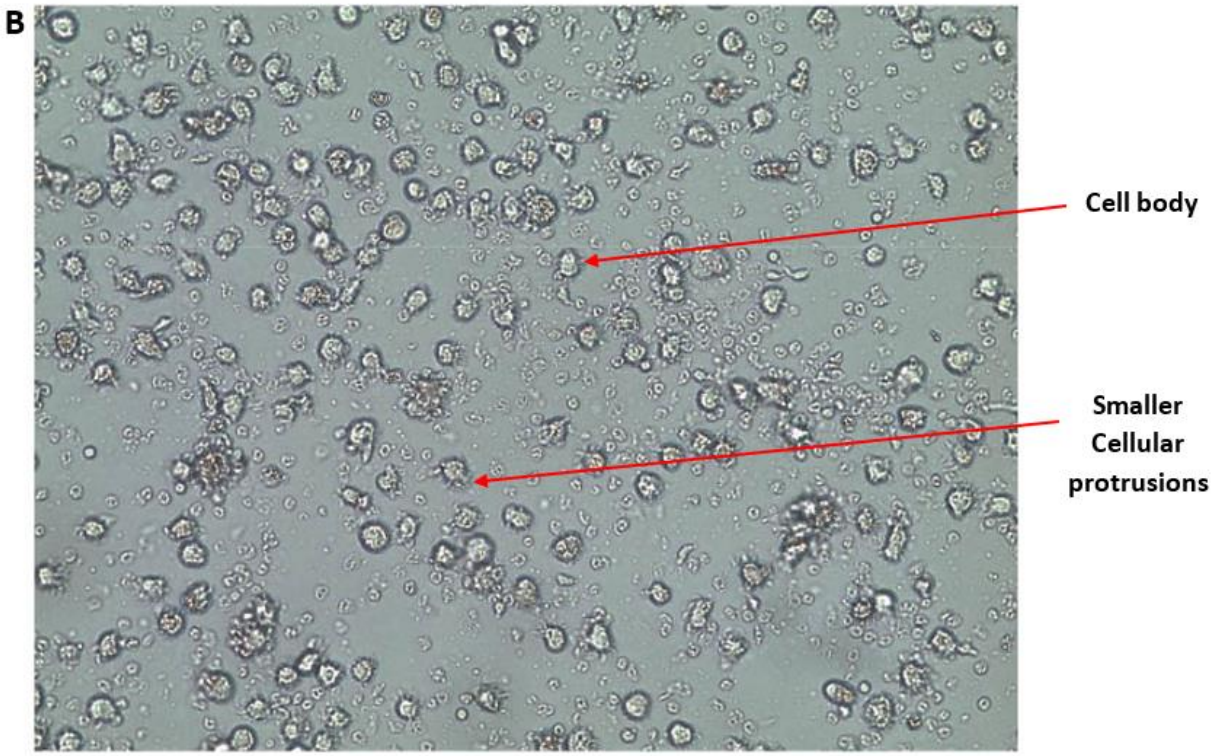

(A) Shows the morphology of the αDC1s which is characterized by the reticulations highlighted by the red arrow denoting cell body and reticulation. (B) Shows the morphology of the DC2s which shows that they are more uniform in size and have smaller reticulations than the αDC1s and is highlighted by the red arrows.

iDCs were stimulated with the different cytokine cocktails mentioned previously and on the seventh day of the culture, prior to harvest, the DCs were imaged and assessed for morphologic differences based on polarization. The αDC1s are characterized by their long cellular protrusions leading to their adherence to the plate. They also are more variable in their shape and size due to the randomness of their protrusion. This can be observed in Figure 3A. The DC2s are more uniform in size and have much smaller cellular protrusion. (Figure 3B). The DC2s are also much less adherent to the plate upon harvesting due to the lack of the larger reticulations that are seen in the αDC1s.

5.1.2 Phenotypic Characterization of Differentially Polarized DC

Polarization was determined using previously described methods involving a cocktail of cytokines. iDCs, which were used as a baseline, were cultured with just GM-CSF and IL-4 for the entirety of the culture. The DCs were phenotypically analyzed for surface markers that are predominantly expressed on DCs. The gating strategy, seen in figure 4A&B shows the cells gated first on the DC population (figure 4A) and second to exclude the doublets recorded while running the flow cytometer. (figure 4B). Immature DCs are characterized by their expression of CD83 and CD86 but a lack of expression in the other markers. (Figure 4C) Meanwhile the αDC1s are characterized by high expression of CD86 and CD83 along with minimal expression of CCR7 and high levels of Siglec-1 while showing low to no expression of OX40L. (Figure 4C). DC2s are characterized by the sample expression of CD83, CD86, and CCR7 while having low levels of Siglec-1 and high levels of OX40L. (Figure 4C)

Figure 4: Different polarization cocktails lead to different phenotypically expressed markers

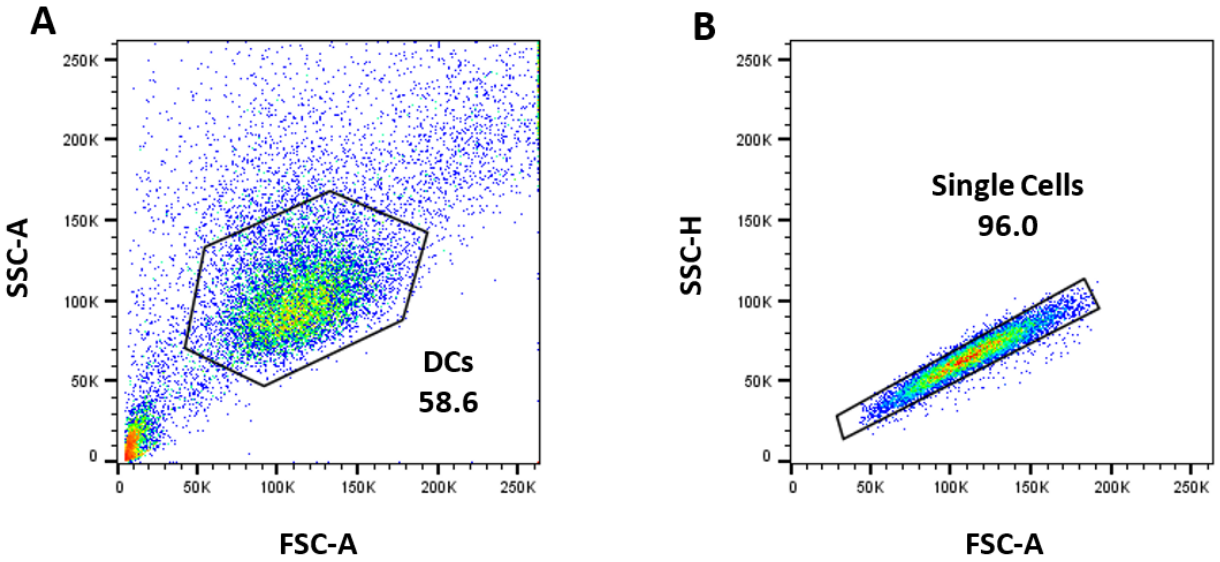

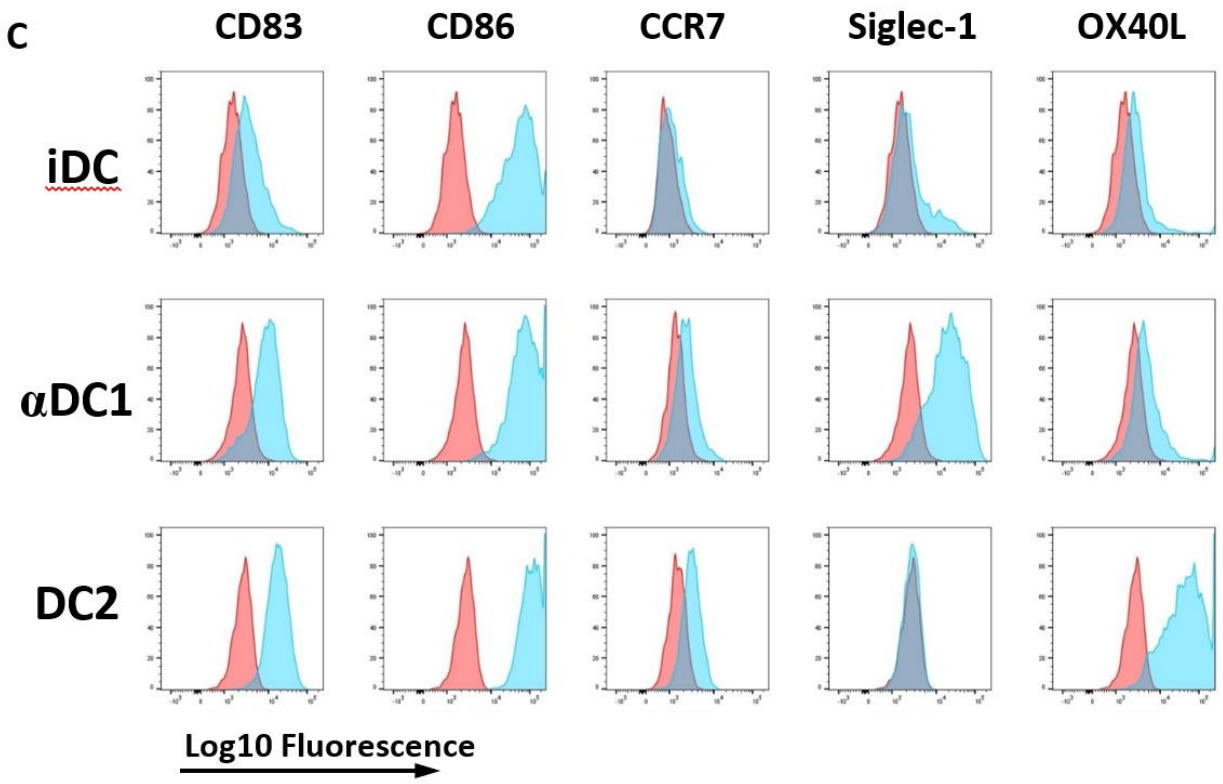

(A) Displays the gating strategy used for the analysis of DCs that were harvested on day 7 of the culture. The gate shown in (A) represents the grouping of dendritic cells used for analysis while (B) shows the grouping of Single cells used for analysis. (C) Red represents the unstained set of cells and blue represents the cells stained with the respective antibody. The x-axis depicts Log(10) of fluorescence and the why axis represents the expression normalized by mode.

Polarization was determined using previously described methods involving a cocktail of cytokines. iDCs, which were used as a baseline, were cultured with just GM-CSF and IL-4 for the entirety of the culture. The DCs were phenotypically analyzed for surface markers that are predominantly expressed on DCs. The gating strategy, seen in figure 4A&B shows the cells gated first on the DC population (figure 4A) and second to exclude the doublets recorded while running the flow cytometer. (figure 4B). Immature DCs are characterized by their expression of CD83 and CD86 but a lack of expression in the other markers. (Figure 4C) Meanwhile the αDC1s are characterized by high expression of CD86 and CD83 along with minimal expression of CCR7 and high levels of Siglec-1 while showing low to no expression of OX40L. (Figure 4C). DC2s are

characterized by the sample expression of CD83, CD86, and CCR7 while having low levels of Siglec-1 and high levels of OX40L. (Figure 4C)

5.1.3 Single Cell Analysis of DC Subsets

Figure 5: The interaction of DCs with CD40L causes change in RNA expression at the single cell level

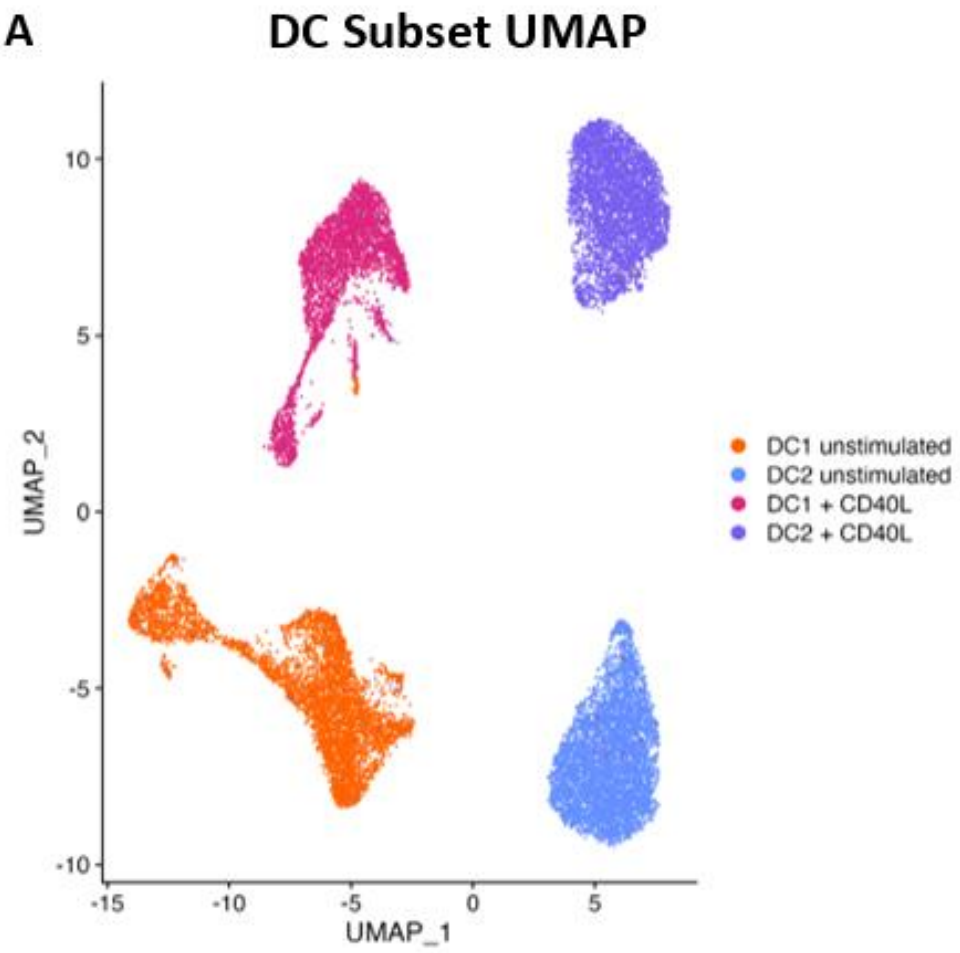

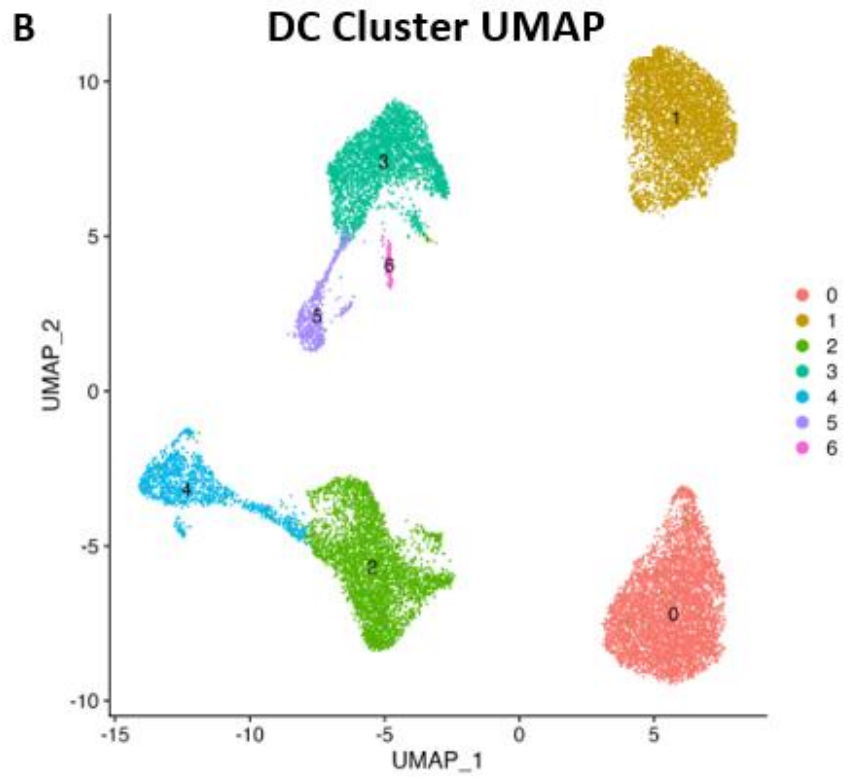
B
DC Cluster UMAP
UMAP_2
UMAP_1
10
5
0
-5
-10
-15
-10
-5
0
5
0
1
2
3
4
5
6

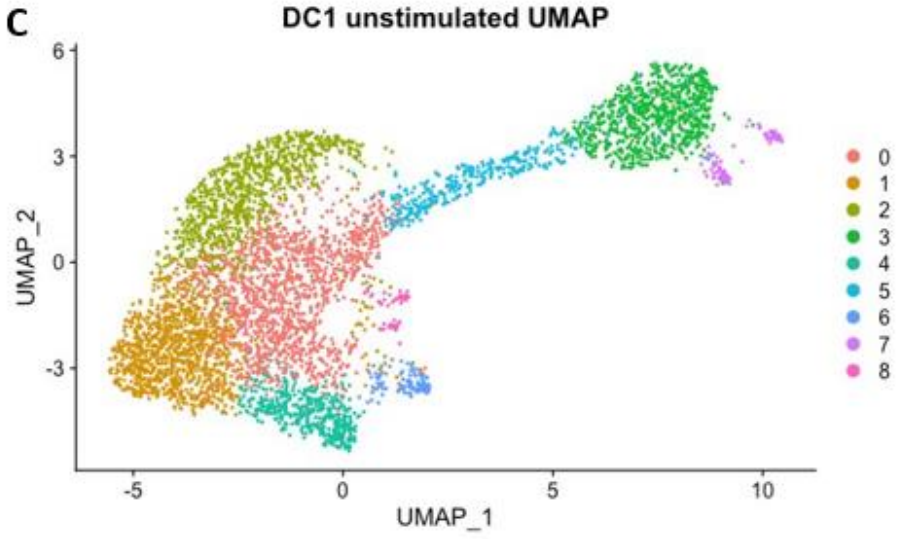
C
DC1 unstimulated UMAP
UMAP_2
UMAP_1
6
3
0
-3
-5
0
5
10
0
1
2
3
4
5
6
7
8

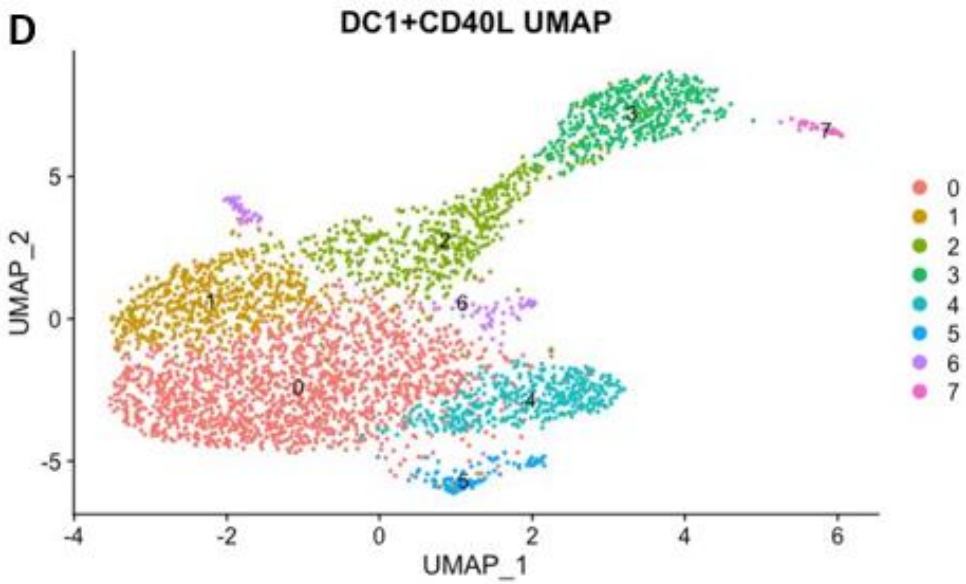
D
DC1+CD40L UMAP
UMAP_2
UMAP_1
5
0
-5
-4
-2
0
2
4
6
0
1
2
3
4
5
6
7

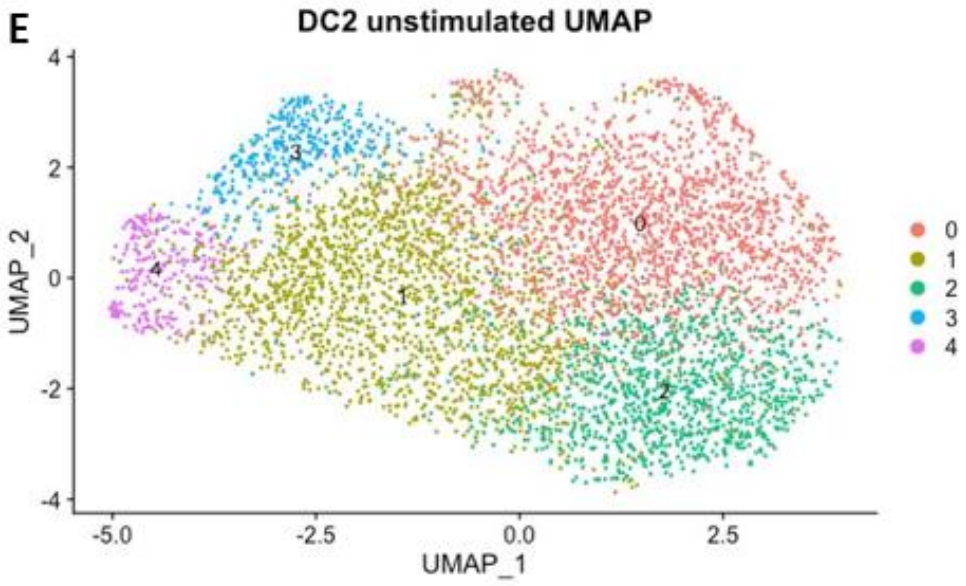
E
DC2 unstimulated UMAP
UMAP_2
UMAP_1
4
2
0
-2
-4
-5.0
-2.5
0.0
2.5
0
1
2
3
4

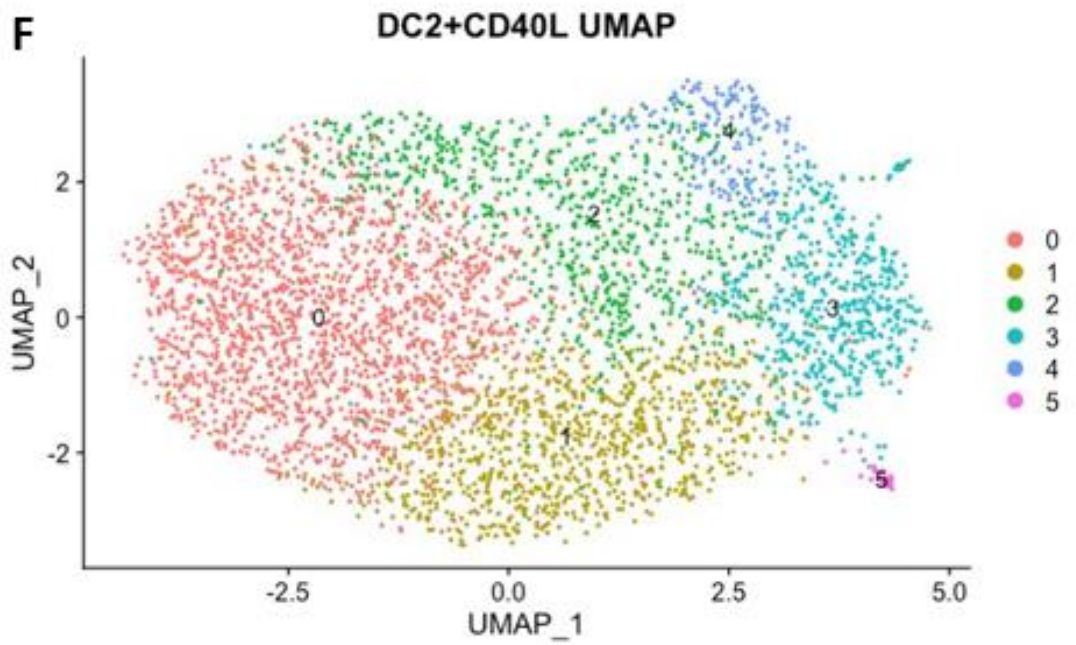

(A) Displays a UMAP of the different subsets of dendritic cell with and without stimulation from CD40L. (B) Displays a UMAP cluster analysis that identifies the different clusters broadly seen between the different population of DCs with and without CD40L. (C) Displays a UMAP cluster analysis of different DC subsets seen within the unstimulated αDC1 population. (D) Displays a UMAP cluster analysis od different DC subsets seen within the αDC1+CD40L population. (E) Displays a UMAP cluster analysis of different DC subsets seen within the unstimulated DC2 population. (F) Displays a UMAP cluster analysis of different DC subsets seen within the unstimulated DC2+CD40L population.

Differentially polarized DC (αDC1 and DC2) were stimulated CD40L on day seven of the culture for 4 hours and then analyzed for difference in RNA expression using single cell whole genome sequencing. A uniform manifold approximation and projection (UMAP) was used to analyze the data. A UMAP is a dimensional reduction technique that is used to analyze and visualize data that tends to have high dimensionality. The UMAPs show that there are distinct clusters that are created for each of the four conditions, αDC1, αDC1+CD40L, DC2, and DC2+CD40L. (Figure 5A) Within those individual clusters, there seems to be more variability in the αDC1 clusters than in comparison to that of the DC2s. (Figure 5B) This can be observed by not only the shape of the clusters, but also by the different number of subpopulations that were

identified by the UMAP data analysis. αDC1 without stimulation had a total of 8 different subpopulations within its cluster (Figure 5C) and αDC1+CD40L had 7 different subpopulations within its cluster (Figure 5D). DC2 without stimulation had 4 subpopulations in its cluster (Figure 5E) and DC2+CD40L had 5 subpopulations. (Figure 5F)

5.1.4 Proinflammatory Cytokine Production in DCs

Dendritic cells were analyzed for their production of various cytokines both with and without stimulation from CD40L from two different sources. Those sources were rhCD40L and stimulation with J558 cells transfected to produce CD40L. This was done through two different Mesoscale Discovery kits that were previously mentioned. In concordance with previous literature, the αDC1s that were stimulated with CD40L produced the highest amount of proinflammatory cytokines compared to all of the DC2 subsets in IL-12p70 (Figure 7A), IL-6 (Figure 6A), IL-18 (Figure 6B), TNF-α (Figure 6C), CXCL10 (Figure 6D), and MIP-1α (Figure 6E). It is important to note that in figure 4E, the DC2s do have some CXCL10 produced, but it is so minute that it is not visible in comparison to the αDC1 groups.

Figure 6: αDC1s produce more proinflammatory cytokines with CD40L stimulation than DC2s in all conditions

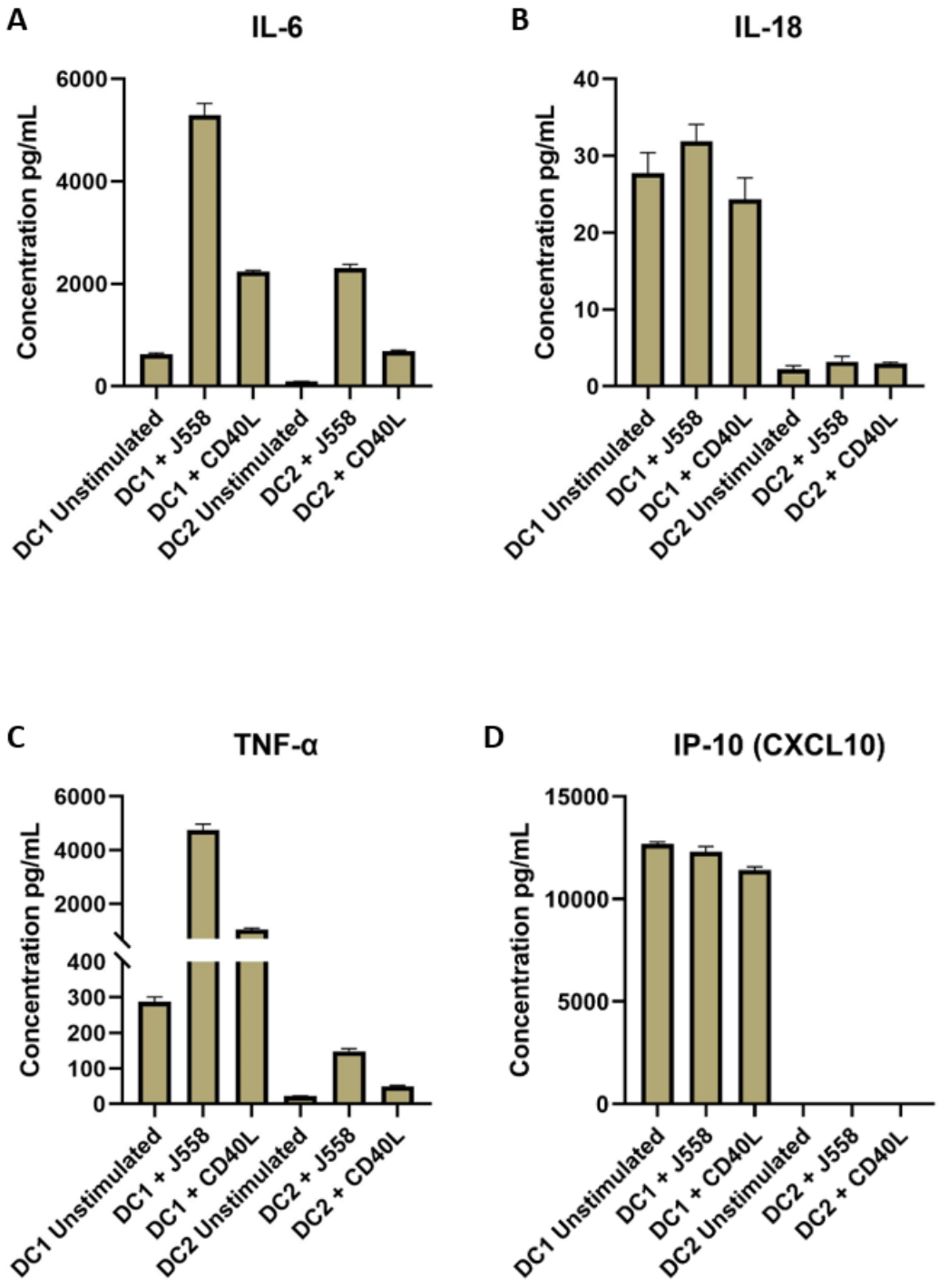

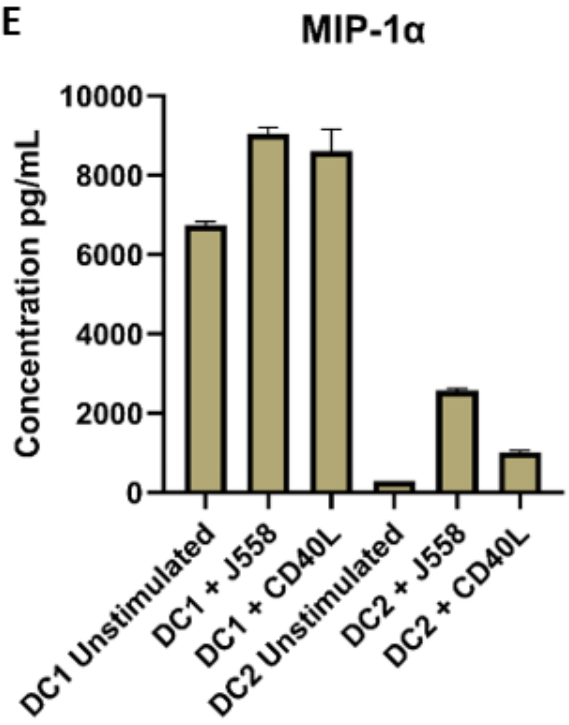

The graphs in figure 6 display the concentration of cytokine in pg/mL of supernatant of each of the 6 condition types: αDC1 unstimulated, αDC1 stimulated with J558 cells, αDC1 stimulated with CD40L, DC2 unstimulated, DC2 stimulated with J558 cells, and DC2 stimulated with CD40L. (A) IL-6, (B) IL-18, (C) TNF-α, (D) CXCL10, and (E) MIP-1α.

Dendritic cells were analyzed for their production of various cytokines both with and without stimulation from CD40L from two different sources. Those sources were rhCD40L and stimulation with J558 cells transfected to produce CD40L. This was done through two different Mesoscale Discovery kits that were previously mentioned. In concordance with previous literature, the αDC1s that were stimulated with CD40L produced the highest amount of proinflammatory cytokines compared to all of the DC2 subsets in IL-12p70 (Figure 7A), IL-6 (Figure 6A), IL-18 (Figure 6B), TNF-α (Figure 6C), CXCL10 (Figure 6D), and MIP-1α (Figure 6E). It is important to note that in figure 4E, the DC2s do have some CXCL10 produced, but it is so minute that it is not visible in comparison to the αDC1 groups.

5.1.5 Higher Production of IL-12p70 in αDC1 is Reflected in Single Cell RNA Expression

Figure 7: A subset within the αDC1 is responsible for a large majority of the IL-12p70 production

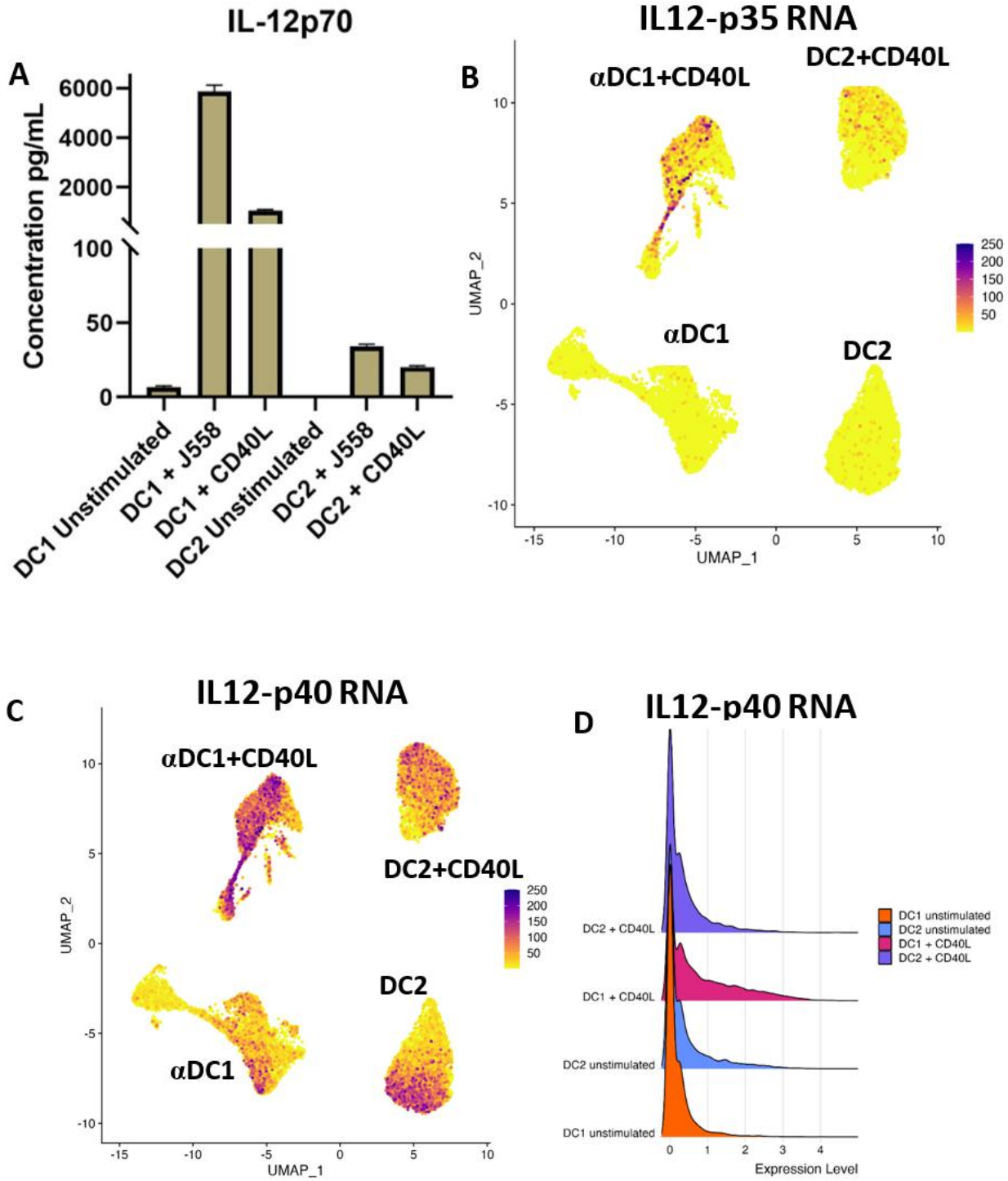

Using the same data from the MSD analysis above, IL12p70 production was measured for the different DC conditions (Figure 7A). This was then compared to the single cell sequencing data looking specifically at the gene encoding IL-12p35 (Figure 7B) and IL-12p40 (Figure 7C), which are both required for an active IL-12p70 cytokine. Looking at both IL-p35 and IL-12p40 allows for the analysis of which subpopulation of αDC1s are responsible for producing the active IL-12p70. The UMAP and a ridge plot graphing fold expression shows a small subset of the αDC1 is producing IL-12p35 and that IL-12p40 is produced relatively equally among the different conditions. (Figure 7D)

5.1.6 The Production of Anti-inflammatory Cytokines in Different DC Conditions

Figure 8: αDC1s produce larger amounts of anti-inflammatory cytokines than DC2s with or without CD40L

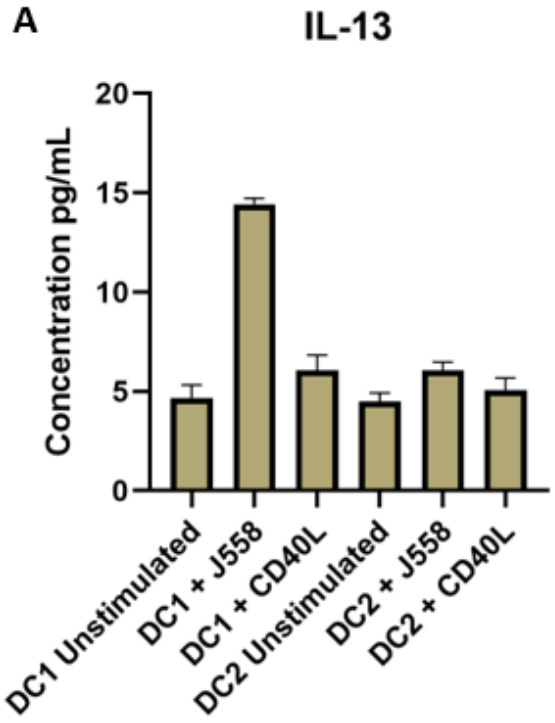

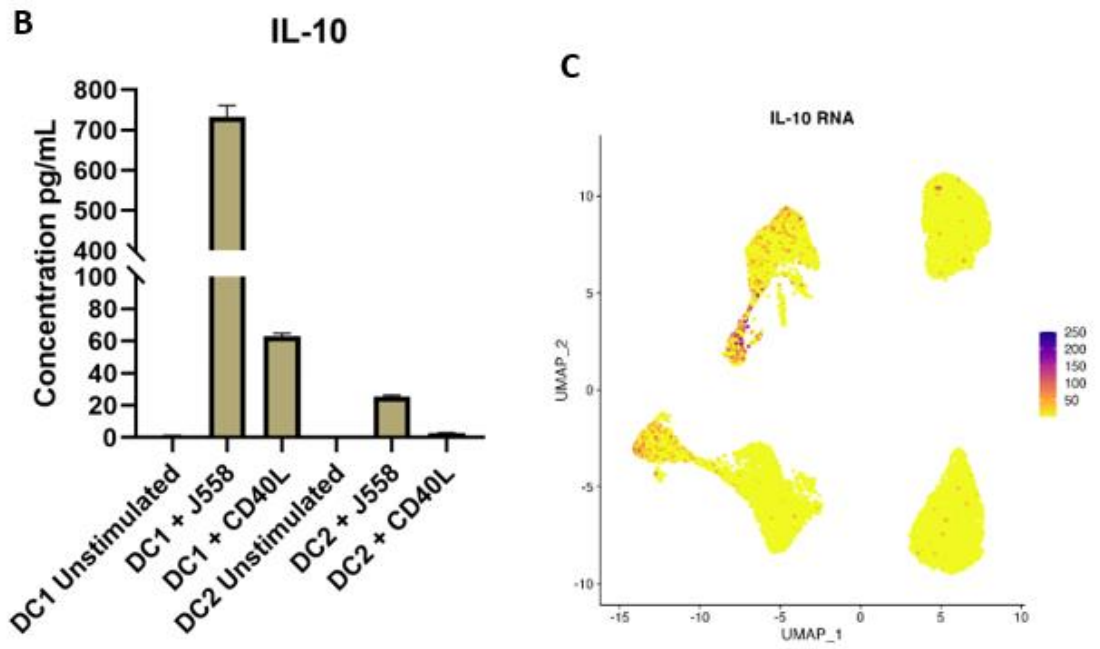

(A) Depicts the IL-13 production in pg/mL within the supernatant of differentially polarized DCs stimulated with rhCD40L and J558 cells. (B) Depicts the IL-4 production in pg/mL within the supernatant of differentially polarized DCs stimulated with rhCD40L and J558 cells (C) Depicts the IL-10 production in pg/mL within the supernatant of differentially polarized DCs stimulated with rhCD40L and J558 cells.

Dendritic cells were analyzed for their production of various cytokines both with and without stimulation from CD40L from two different sources. Those sources were rhCD40L and stimulation with J558 cells transfected to produce CD40L. Traditionally, αDC1s are known to drive a more proinflammatory response while DC2s tend to release more cytokines that drive an anti-inflammatory response or a T_H1 response. However, when we analyzed αDC1s and DC2s with and without stimulation, it showed that the αDC1s produce higher amounts of anti-inflammatory cytokines IL-13 (Figure 8A), and IL-10 (Figure 8B). This was an unexpeted finding from the MSD data. Figure 8C shows IL-10 RNA expression from the single cell data.

5.2 Aim 2: The Isolation and Characterization of DC-Derived EVs from Differentially Polarized Dendritic Cells (αDC1, and DC2)

5.2.1 Isolation of Extracellular Vesicles from DCs

Figure 9: Devised EV isolation protocol

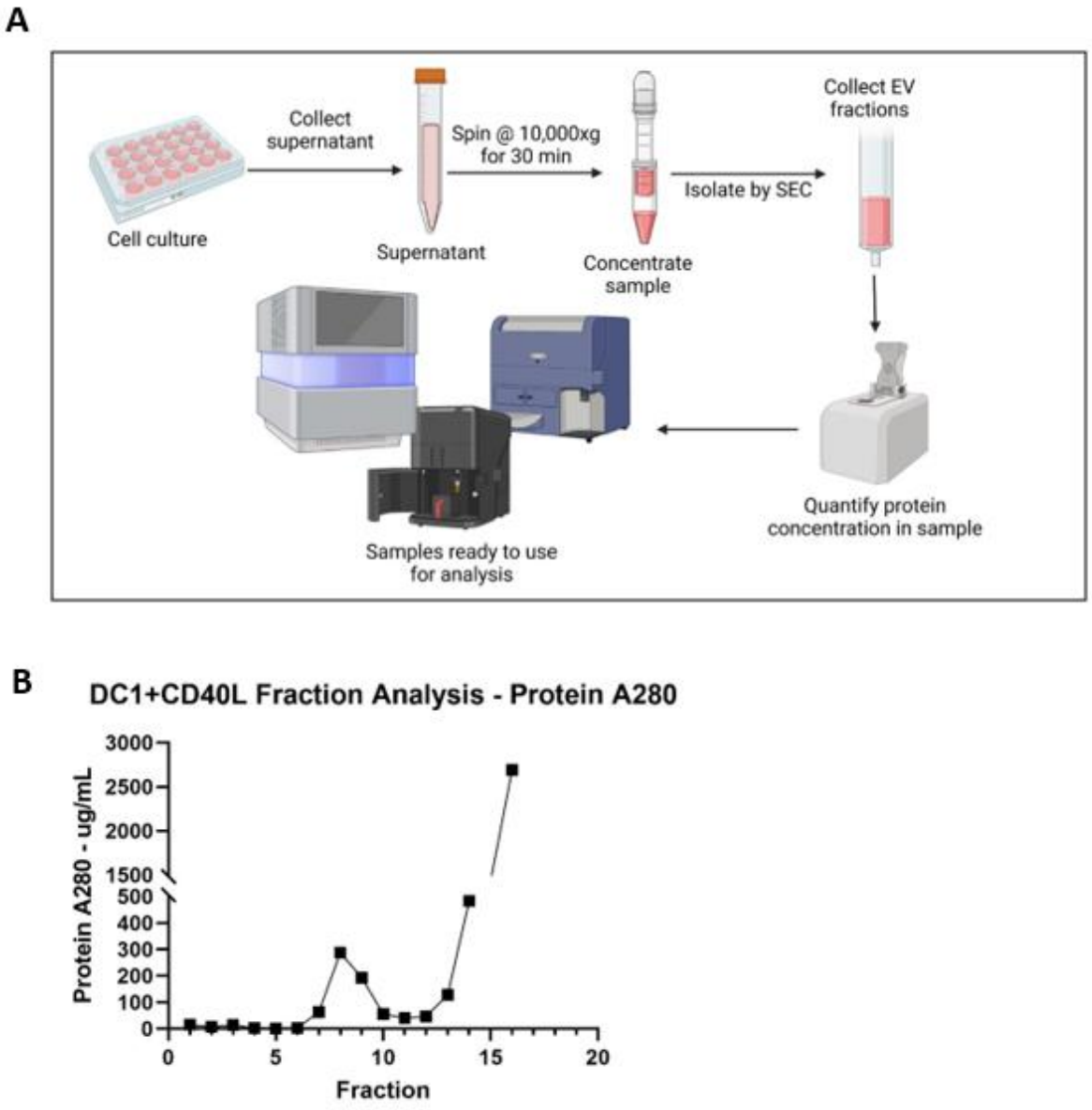

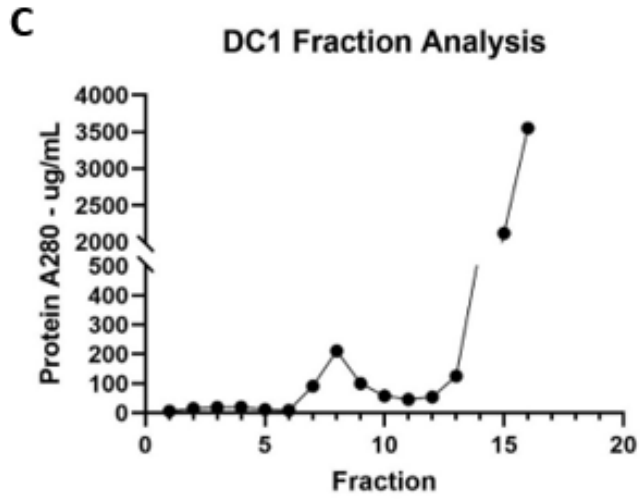

(A) Describes the protocol used to isolate extracellular vesicles in the Milliard Lab for further analysis. Image was created using BioRender. (B) & (C) Display the amount of protein recorded in each of the fractions collected from the αDC1 condition and the αDC1+CD40L condition respectively.

A big challenge during this process was creating a protocol for the isolation of EVs from the cell culture supernatant of DCs. Common methods of EV isolation require large amounts of supernatant and require the usage of an ultracentrifuge, which spins at a speed of 100,000 x g for long periods of time. The ultracentrifuge harbors some of the more standard protocols for the isolation of EVs such as density gradient centrifugation and traditional ultracentrifugation. These methods work well with large sample sizes such as 100mL plus of sample. In our lab, this is not a feasible amount of cell culture supernatant to work with; we worked with around 6mL of supernatant at the time. The procedure that was derived for the isolation of EVs from DC cultures in the Milliard Lab used a process of sample concentration using a protein concentrator and size exclusion chromatography. The protocol can be followed in Figure 9A. Upon the harvest, the first spin was used to exclude any cellular material or debris in the sample. The second spin, using a high-speed centrifuge at 10,000 x g was used to cause the microvesicles to fall out of solution. The sample was then placed in a 100kDa protein concentrator. This allowed for anything smaller than

100kDa, i.e. any residual proteins that may be the same size as the target EVs but a different molecular weight, to pass through the column allowing for 6mL of cell culture supernatant to be concentrated into 500uL of EV sample. This then was passed through IZONs qEV original column to elute out the specific EV fractions that could be concentrated for further analysis. These fractions were determined by taking the protein concentration in pg/mL in each of the fractions collected using a Nanodrop. These data were then graphed to find the point at which the first peak in protein concentration is observed (Figure 9B&C). These fractions were then kept and pooled while the others were discarded. The EV fraction peak typically forms around the seventh, eighth, and nineth fraction.

5.2.2 Characterization of Extracellular Vesicles by Size

Figure 10: Both polarization and stimulation with CD40L cause differences between DC conditions

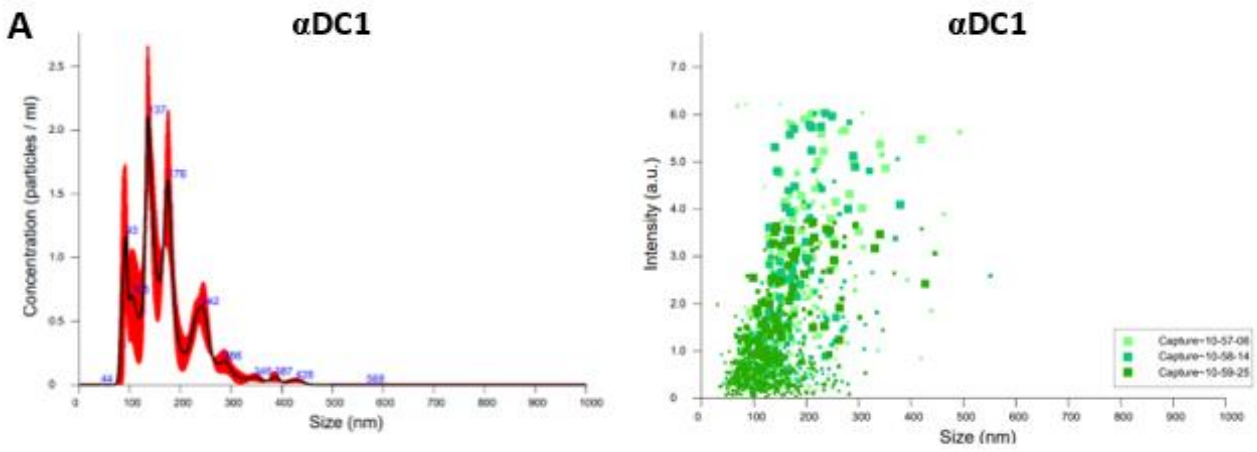

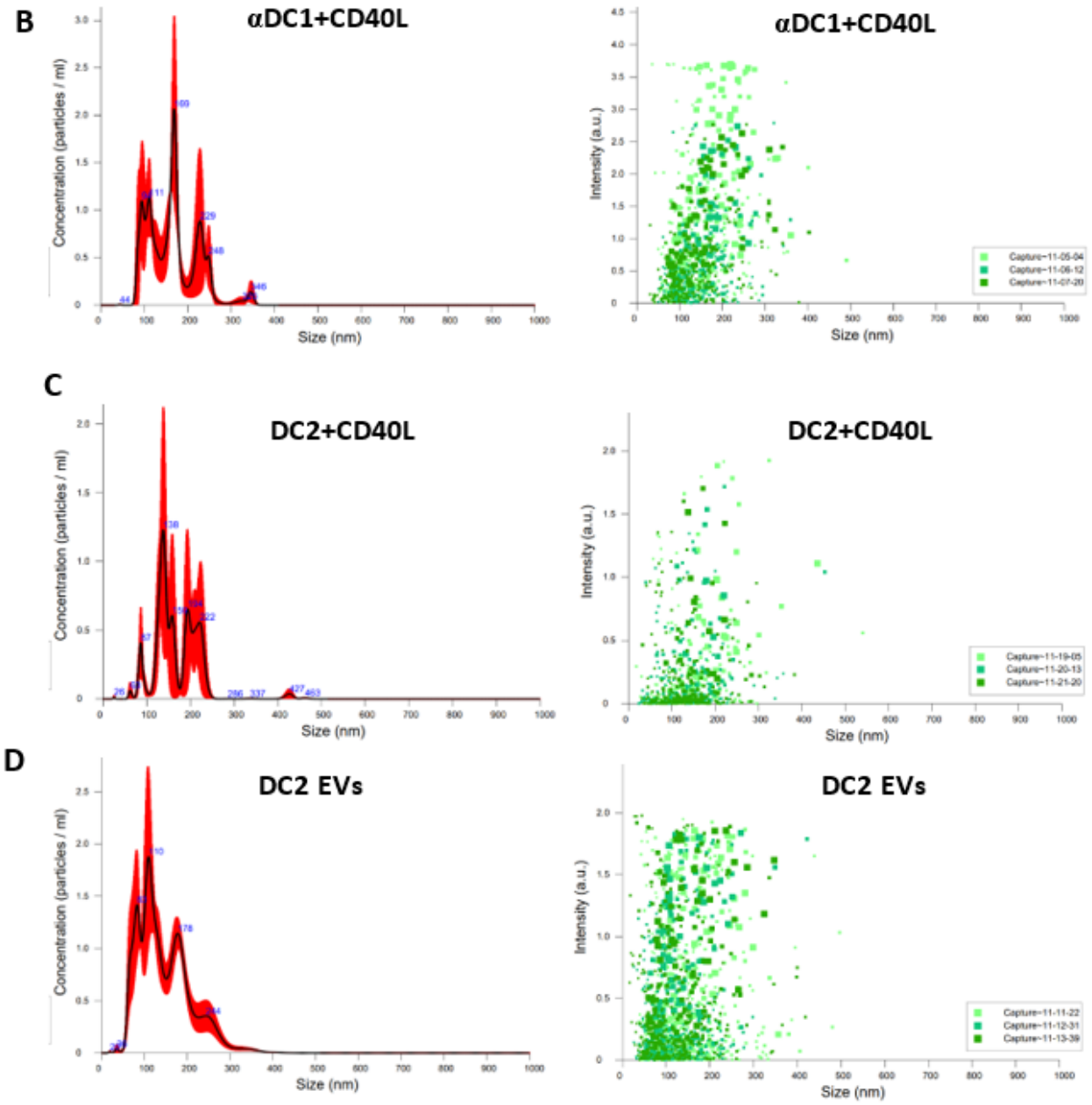
B
αDC1+CD40L
Concentration (particles / ml)
Size (nm)
αDC1+CD40L
Intensity (a.u.)
Size (nm)
Capture-11-05-04
Capture-11-06-12
Capture-11-07-20
C
DC2+CD40L
Concentration (particles / ml)
Size (nm)
DC2+CD40L
Intensity (a.u.)
Size (nm)
Capture-11-19-05
Capture-11-20-13
Capture-11-21-20
D
DC2 EVs
Concentration (particles / ml)
Size (nm)
DC2 EVs
Intensity (a.u.)
Size (nm)
Capture-11-11-22
Capture-11-12-31
Capture-11-13-39

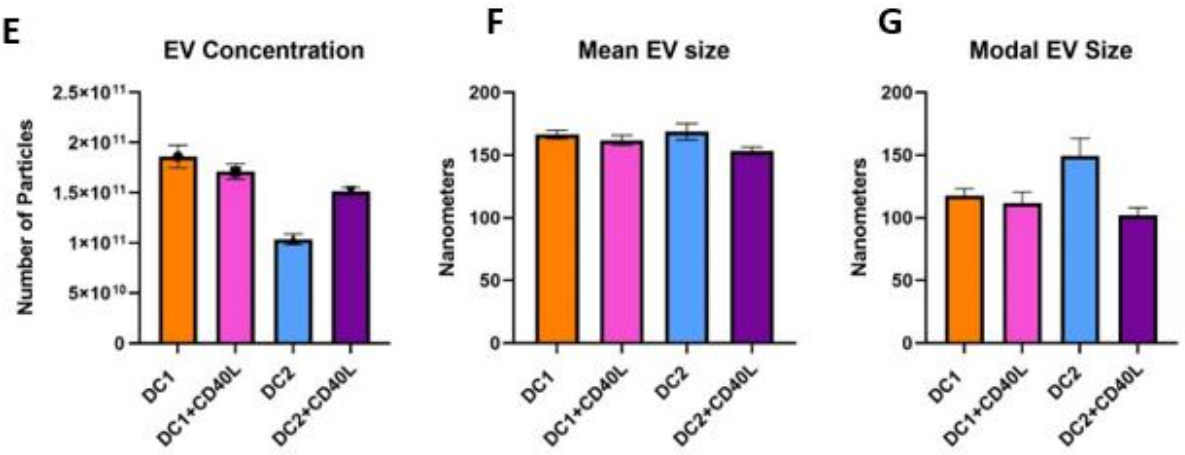

(A) The graph displays the nanoparticle tracking analysis data averaged over the course of three runs for the αDC1 EVs. (B) The graph displays the nanoparticle tracking analysis data averaged over the course of three runs for the αDC1+CD40L EVs. (C) The graph displays the nanoparticle tracking analysis data averaged over the course of three runs for the DC2 EVs. (D) The graph displays the nanoparticle tracking analysis data averaged over the course of three runs for the DC2+CD40L EVs. (E) The bar graph depicts the differences in concentration of particles based on condition. (F) This bar graph compares the mean size of EV isolated from each of the different conditions. (G) This bar graph compares the modal size of EV isolated from each of the different conditions.

DC-derived EVs were isolated from the cell culture supernatant of dendritic cells that were cultured in serum-free media (AIM-V). The supernatant was collected on day 7 after a 24hr stimulation of rhCD40L. EVs were isolated from αDC1, αDC1+CD40L, DC2, and DC2+CD40L cultures. Size analysis of the EVs was determined through nanoparticle tracking analysis which denotes the size of individual vesicles using a laser and observing the scattering of the light in terms of its Brownian motion. The graphs depicted display the size as an average of three different trials, and each of the peaks seen in the graph are a cluster of EVs ranging in similar size. Along with that, a graph of intensity vs. size is given for each of the samples which shows the size where the majority of EVs are located. (Figure 10A, 10B, 10C, and 10D) Using this technique, EVs can be observed on an individual basis and a concentration can be determined. (Figure 10E) The samples were diluted 1:500 when the sample was run and the concentration of EVs in each sample was calculated accordingly. What can be seen is that the conditions that were stimulated with

CD40L had a smaller EV size, which is observed in both the mean (Figure 10F) and modal (Figure 10G) distribution.

5.2.3 Flow Cytometry Analysis of EVs

Figure 11: Expressional Analysis of traditional EV markers using bead-based flow cytometry

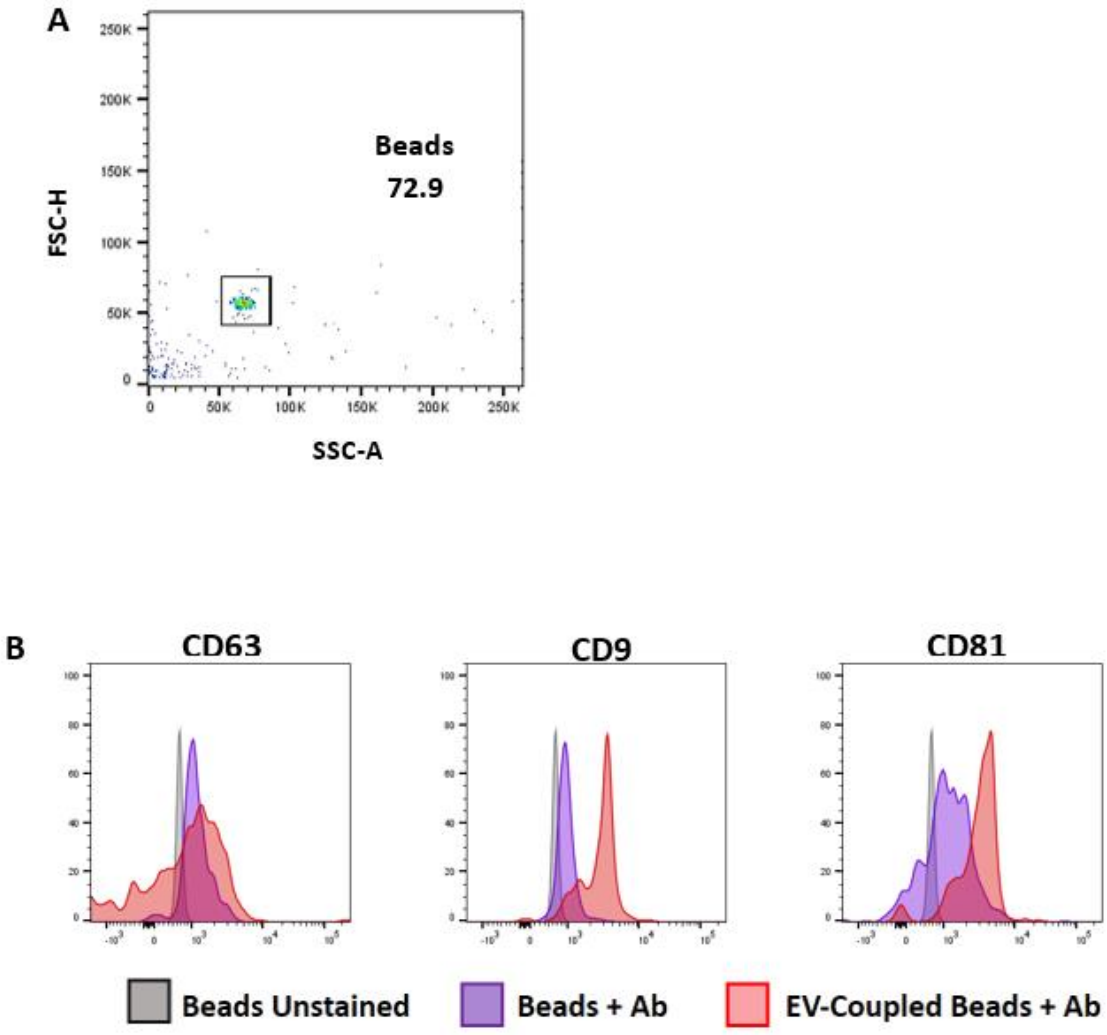

(A) This figure displays the gating strategy for the analysis of EV-bead complexes via flow cytometry. (B) This figure displays the expression of markers CD63, CD9, and CD81 on EV-bead complexes using flow cytometry.

As a means to verify the presence of EVs in our samples, a flow cytometry-based assay was used to phenotypically characterize the EVs for common surface proteins CD9, CD63, and CD81. Beads are required to be used because the size of the EVs is too smally for the cytometry to detect. To circumvent this, using a bead-based model allowed for the EVs to still be analyzed but the actual item the cytometer was using for analysis was within the size range for the cytometer's detection. So specifically, the samples were incubated with the CD63 isolation beads by Dynal overnight on a shaker, in a cold room to allow the EVs to bind to the beads based on their presence of CD63. This is one of the most common EV markers, so it is a good target for the bead-based assay. The EV-bead complexes were then stained for markers CD63, CD81, and CD9. The beads were gated based on the singlets of the beads, excluding any debris or doublets that were recorded. (Figure 11A) This model proved challenging, as it only was successful part of the time, which led to minimal usable data. However, when it was successful, the expression of CD63 was low, possibly due to saturation of the EVs with the beads, CD9 and CD81 expression was high. (Figure 11B) The graph depicts three different peaks, the beads unstained, the beads with the EVs, and the beads, EVs and stains.

5.2.4 Using Single Cell Sequencing Data to Analyze the Effect of CD40L Stimulation of DCs on EV Regulation Related Factors at the RNA Level

Figure 12: CD40L causes an increase in expression of EV genes that are important for EV production and release

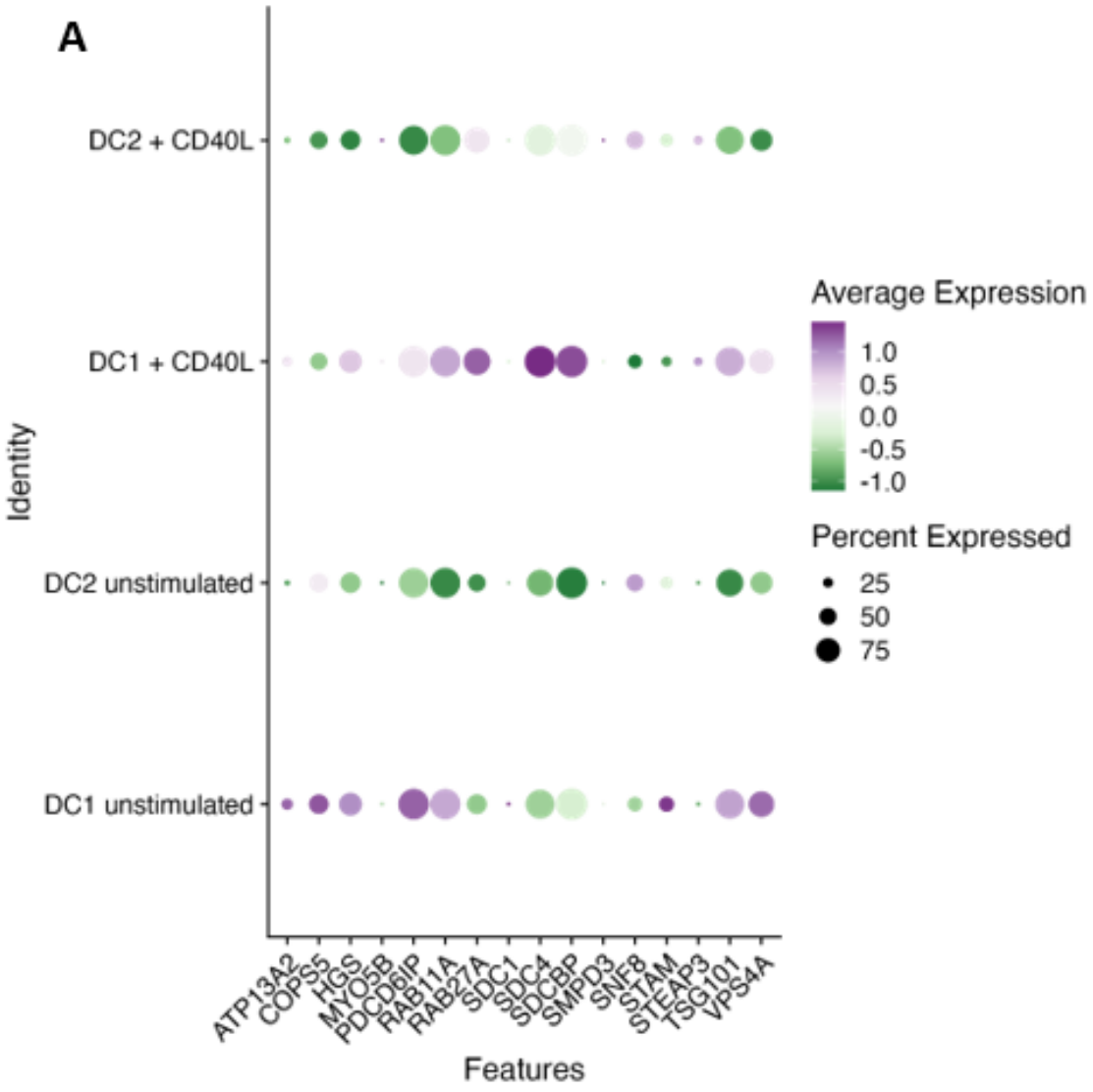

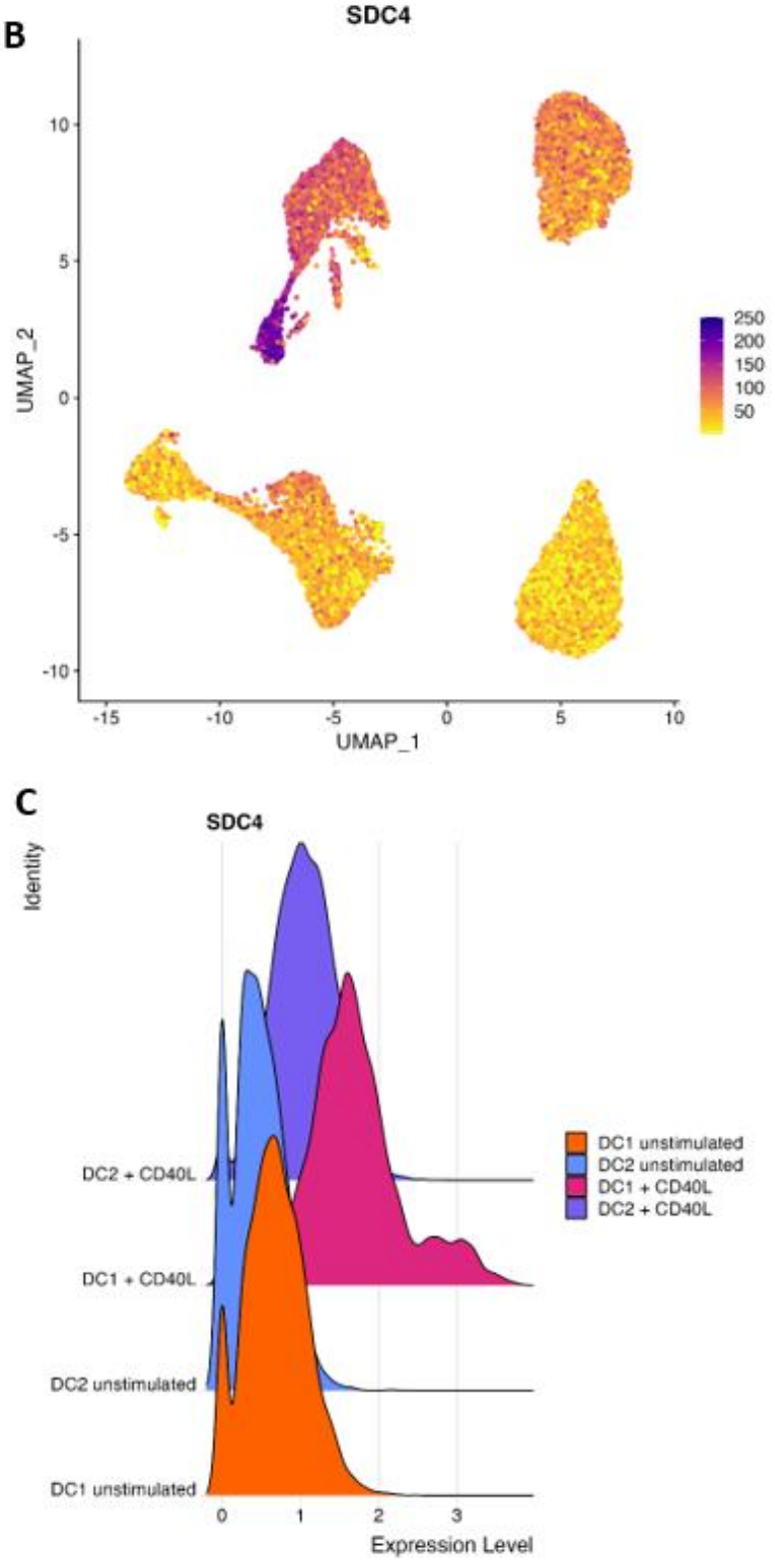
B
SDC4
UMAP_2
UMAP_1
10
5
0
-5
-10
-15
-10
-5
0
5
10
250
200
150
100
50
C
SDC4
Identity
DC2 + CD40L
DC1 + CD40L
DC2 unstimulated
DC1 unstimulated
0
1
2
3
Expression Level
DC1 unstimulated
DC2 unstimulated
DC1 + CD40L
DC2 + CD40L

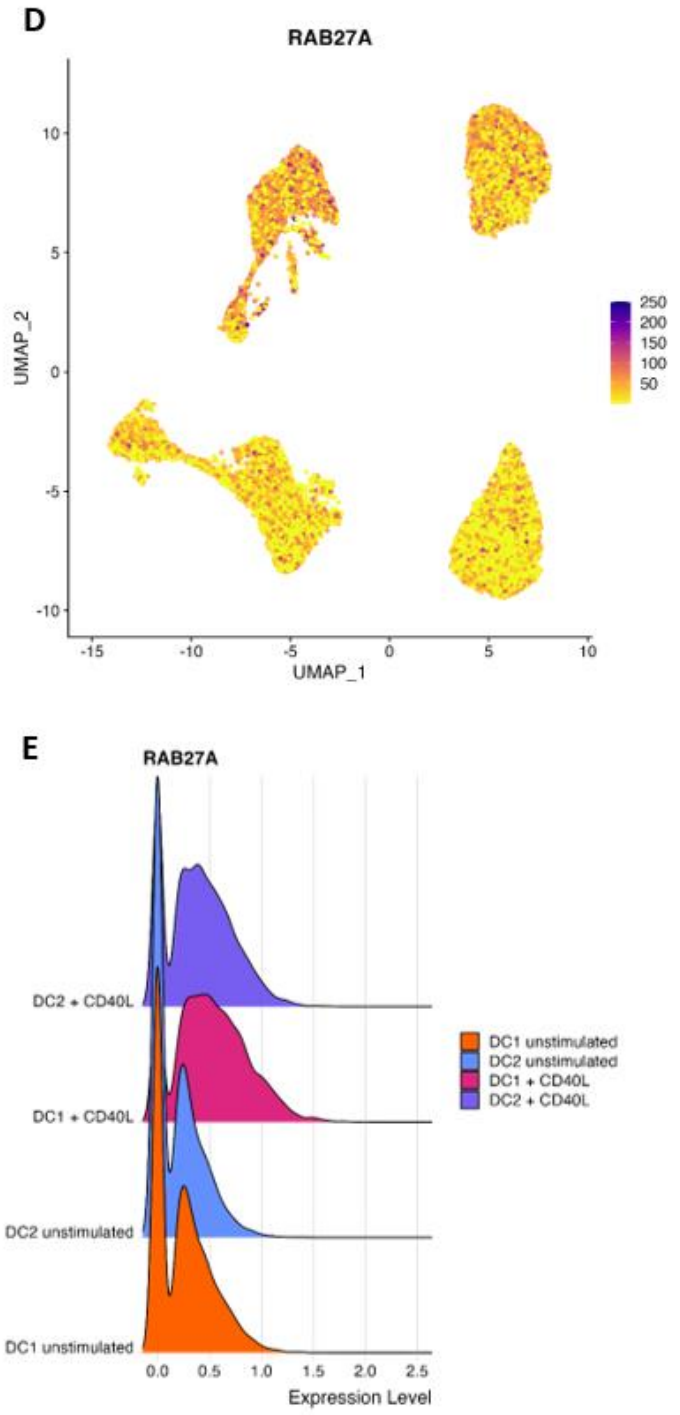

(A) A Dotplot analysis showing a change in expression and in the number of cells within the population expressing the gene. (B) A UMAP analysis of SDC4 as its expression is compared among different DC conditions. (C) A ridge plot displaying the change of expression level between DC conditions. (D) A UMAP analysis of RAB27A as its expression is compared among different DC conditions. (E) A ridge plot displaying the change of expression level between DC conditions.

Using the single cell sequencing data from the first aim, we were able compare the RNA expression of genes that code for extracellular vesicle relevant proteins between the different polarization types with or without CD40L stimulation. A dot plot depicting the changes in expression of a panel of EV relevant genes is characterized by two different styles of change. (Figure 12A) A color change in the figure denotes a change in RNA expression while a change in size related to the percentage of cells within the given population that are expressing the particular gene of interest. This dot plot shows that with stimulation of CD40L, there is an increase in expression of several different markers in both the αDC1 conditions and when looking at specific genes such as SDC-4 (Figure 12B and 12C), RAB27A (Figure 12D and 12E) The αDC1 conditions had a higher expression of those genes in comparison to the DC2s and the αDC1s stimulated CD40L had the most expression out of any of the different conditions. In each of those examples there are different subsets within the αDC1 conditions that are expressing each particular gene at a higher rate than their counterparts. This section of cells with the αDC1 conditions has become an area to focus upon as a possible subset of αDC1s that are hyperactivated in comparison to the rest.

6.0 Discussion

DCs play such an integral role in the immune system as they serve as the communicator between the innate and the adaptive arms. As professional APCs, their role in the uptake and presentation of antigen to the T cell is a critical aspect in the success or failure of the immune system. Without it, the immune system would lack consistency and efficacy. [11] This function is also why DCs are the focus of so many different therapeutics in research. Work previously show by Kristoff et.al showed that αDC1 stimulated with CD40L were able to reverse latency in the infected cells making DCs a potential latency reversal agent in the 'kick and kill" model of therapeutics. [9] Adding to that, the work of Garcia-Bates et.al showed that antigen loaded αDC1 were able to create a HIV specific CTL response against sub-dominant and highly conserved regions of HIV, thus satisfying the "kill" mechanism of the "kick and kill" model. [23] Work by Zaccard et.al pointed out major differences between αDC1 and DC2 when stimulated with CD40L such as tunneling nanotube formations, higher IL-12p70 production and what appeared to be exosomal release of cellular material, all of which that pointed to αDC1 as being the more biologically functional DC type for this "kick and kill" concept, despite DC2s being the primary DC type in clinical trials currently. [10] Taking all of this into account, it was imperative to develop a deep understanding of the differences between the DC types and the extracellular vesicles they produce so that our knowledge of the DC type could help to create a more functional and novel therapeutic.

My first aim was the deep characterization of the αDC1 and DC2 subtypes with and without stimulation from CD40L. In Figure 3A and 3B it can be seen the stark differences in morphology of the DCs. The αDC1s have long cellular protrusions that are used for communication with

different cell types. They also can be noted as being much less uniform in structure than the DC2. When moving onto the phenotypic analysis (Figure 4) of the DC types we saw much higher levels of expression in Siglec-1 in the αDC1s and much higher levels of expression of OX40L in the DC2. OX40L is a co-stimulatory molecule among the same family as CD40L. It plays a role in Signal 2 and drives a Th2 response. Both DC types expressed CD83 and CD86 and minimally CCR7. These two figures are standards for our lab in working with DCs. Figure 5 is the single cell analysis of the DCs. When the data were analyzed, it created 4 distinct regions that were denoted as each condition. This was good to see because it showed that the maturation factors were successful in creating differentially polarized dendritic cells, and that there was a difference in RNA expression when the DCs are stimulated with CD40L, further supporting the idea that CD40L is key in the hyper-activation of DCs. What is important to note are the different clusters seen in figure 5B and highlighted in figures 5C-E. In a UMAP, the grouping created are based on the similarities of the items in the cluster. The more homogenous the cluster, the more similar all the cells were. What we see in the αDC1s are a wider variety of clusters, suggesting that there are subsets within the cluster of αDC1s that matured differently from some of their neighbor cells.

Next, we looked at the pro-inflammatory cytokine production (Figure 6) from the different DC conditions using MSD. What was noted was that αDC1s were higher producers of pro-inflammatory cytokines. This is what was expected to be seen as αDC1s are known to drive a Th1 response and DC2s are known to drive a Th2 response. We also saw that when stimulated with CD40L the DCs of both classes created more pro-inflammatory cytokines. Specifically, the DCs stimulated with J558 transfected cells had the highest cytokine production. This is likely due to signal transduction coming from the direct interaction between cells. When stimulated with CD40L alone, the DCs miss some of those costimulatory molecules that would help to drive a

more robust cytokine response. Knowing that IL-12p70 is produced highly in αDC1s we decided to take the MSD data and compare it to IL-12 production at the RNA level in the single cell data. We noted that the single cell data in fact reflected what was seen in the MSD data. What was particularly interesting was that we saw the inactive subunit IL-12p40 highly expressed at the RNA level in all of the conditions, but only saw a larger expression of the Il-12p35, the active subunit of Il-12p70 in the αDC1s, particularly the ones stimulated with CD40L. This fortifies the idea that αDC1s are better at driving a CTL response as IL-12p70 is one of the most potent pro-inflammatory cytokines.

What was seen next was quite surprising. We also decided to look at anti-inflammatory cytokines like IL-10, an IL-13 which are known to be drivers of a Th2 response and typically created more frequently from DC2. What we observed was that the αDC1s were also more effective at producing anti-inflammatory cytokines, this causes us to compare this to the single cell data as well. What we observed what surprising. When looking at IL-10 production (Figures 8C & 8D) we saw that there was low expression of IL-10 RNA everywhere except for a small population with the αDC1s stimulated with CD40L. This same population is the grouping the consistently has some of the highest expression in all of the single cell data, which can be seen in the IL12 graphs (Figure 7) which supports the idea that CD40L creates hyper-activated and overproducing αDC1s. This was one of the most interesting finds from the single cell data.

For my second aim, I was tasked with devising a protocol for the isolation of EVs from DC subsets. I was faced with some immediate challenges such as low sample volumes and not having access to an ultracentrifuge. These two compounded with one another, because even if there was access to an ultracentrifuge, the sample volume I had would not have withstood all of G-forces and I would have been left with very little product, as ultracentrifuging causes a loss of roughly

70% of the sample. [26] The method I settled upon used size exclusion chromatography, a method that elutes based upon size. Although time consuming, the process yielded successful results which I then used for analysis. This protocol is now established for further research in the Mailliard Lab on extracellular vesicles.

First, the EVs were analyzed for size and concentration using a Nanosight and nanoparticle tracking analysis. We observed that when stimulated with CD40L, the DCs created smaller extracellular vesicles based on mean and modal distribution. (Figure 10) All of the samples had peaks in vesicle size at less than 200nm which is congruent with the standard size of the nanoparticles. I then used the EVs for flow cytometry analysis of surface protein markers CD9, CD63, and CD81. This proved to be a challenging model to work with as with low sample volumes it was mildly ambiguous whether the vesicles would adhere to the CD63+ beads. What was observed was that CD63 expression was low, which possibly could have been because of the usage of CD63+ beads saturating the EVs, but in the CD9 and CD81 samples, a strong shift in fluorescence denotes that there was expression of those markers detected in the sample, thus validating that what was isolated was extracellular vesicles.

As the end of my time in the Mailliard Lab rapidly approached, there were inevitably some projects that did not get fully completed. Isolated EVs from each of the discussed conditions were sent for miRNA sequencing to the genomics core at UPMC Children's Hospital, but those results will not be back in time for analysis prior to the writing of this thesis, so I decided to investigate into the single cell data and look at how CD40L stimulation effected the RNA expression of proteins that play a role in EV trafficking. What we observed was that the CD40L stimulated conditions , showed an increased expression of exosomal RNA molecules seen in both the αDC1s and DC2, but at a much larger amount in the αDC1s. (Figure 14A) What was also interesting was

that SDC-4, a protein that is part of the exosomal trafficking system, but also an integral structural protein, is expressed highly in the αDC1s that were stimulated with CD40L, which could correlate to the TNTs that are seen when αDC1s are stimulated with CD40L.

These findings are intriguing and shed light on some of the lesser understood mechanisms that have been seen in the works of Zaccard, Garcia-Bates, and Kristoff. There is still much to deduce from this work, but it also opens up new areas to explore when looking at creating a novel therapeutic. For instance, it is unclear if there are truly different subsets of DCs in the aDC1 cultures, or if they are the expression patterns different due to timing of their harvest. And, if there is only a fraction of the culture having a true DC1 phenotype, is there a way to generate or isolate a more homogenous population for therapeutic purposes? This could lead to a hyper-active DC that is then used as the manifold of the "kick and kill" model in a novel HIV therapeutic. Another realm that could be explored would be determining if DCs could be induced to make specific EVS that could be used to help fortify an aspect of the "kick and kill" model which starts by understanding their interaction with T cells in culture. These questions could be linked to the next big steps in the development of functional of a cure for HIV.

7.0 Public Health Significance

Nearly 37 million people are currently living with HIV and around a million people die every year from it. [1] As we live in the United States with generally good access to healthcare, we tend to forget about how fortunate we are sometimes. HIV continues to plague other parts of the world. The WHO states that in their defined African Region, 1 and 25 adults are currently living with HIV. This means that HIV research is as critical as it can be right now. The dendritic cell is one of the most well studied and diverse cell types in all of the immune system. With that being said, there is still so much to learn about its different functions and the ways they can be utilized to help eradicate the world of HIV. Focusing on the role of αDC1s as the centerpiece to a novel HIV therapeutic is taking the first steps. The single cell sequencing data will be useful in this process as it gives insightful detail to the diversity of the αDC1 population. Along with that, the correlation between the RNA level and the protein level is incredibly important. Using the MSD data and cross-analyzing it with the data from the single cell sequencing will prove to be a beneficial process as we strive to make a novel HIV therapeutic.

The extracellular vesicle field is expanding exponentially. As previously stated, the use of nanoparticles as means of improving drug delivery could be the future of medicine. It has already shown efficacy in LRAs and in ART. [2] Establishing a protocol for the Mailliard lab for EV isolation has now opened the door to further research of not only EVs from DCs, but EVs from CD4+ T cells, and from CTLs. This allows for future students to take protocol and apply it to the work that they do. EVs could even end up playing a relevant role in the “kick and kill” method as means of improving delivery of antigen or by stimulating other immune cells to illicit an even more robust response. Outside of the world of HIV, EVs serve roles as biomarkers in other diseases

such as coronary heart disease, a leading cause of death here in the United States. [5] As more is learned about EVs the increasingly important they will be come to the public health landscape. Therefore, it is an excellent time to get into the field.

Bibliography

1. Rodés B, Cadiñanos J, Esteban-Cantos A, Rodríguez-Centeno J, Arribas JR. 2022. Ageing with HIV: Challenges and biomarkers. eBioMedicine 77.

2. Labh R, Gupta R. 2021. Emerging Trends in the Long-Acting Antiretroviral Therapy: Current Status and Therapeutic Challenges. Curr HIV Res 19:4-13.

3. Archin NM, Margolis DM. 2014. Emerging strategies to deplete the HIV reservoir. Curr Opin Infect Dis 27:29-35.

4. Zerbato JM, Purves HV, Lewin SR, Rasmussen TA. 2019. Between a shock and a hard place: challenges and developments in HIV latency reversal. Curr Opin Virol 38:1-9.

5. Margolis DM, Archin NM, Cohen MS, Eron JJ, Ferrari G, Garcia JV, Gay CL, Goonetilleke N, Joseph SB, Swanstrom R, Turner AW, Wahl A. 2020. Curing HIV: Seeking to Target and Clear Persistent Infection. Cell 181:189-206.

6. Jones RB, O'Connor R, Mueller S, Foley M, Szeto GL, Karel D, Lichterfeld M, Kovacs C, Ostrowski MA, Trocha A, Irvine DJ, Walker BD. 2014. Histone deacetylase inhibitors impair the elimination of HIV-infected cells by cytotoxic T-lymphocytes. PLoS Pathog 10:e1004287.

7. Bowen A, Sweeney EE, Fernandes R. 2020. Nanoparticle-Based Immunoengineered Approaches for Combating HIV. Front Immunol 11:789.

8. Elashiry M, Elsayed R, Cutler CW. 2022. Exogenous and Endogenous Dendritic Cell-Derived Exosomes: Lessons Learned for Immunotherapy and Disease Pathogenesis. Cells 11:115.

9. Kristoff J, Palma ML, Garcia-Bates TM, Shen C, Sluis-Cremer N, Gupta P, Rinaldo CR, Mailliard RB. 2019. Type 1-programmed dendritic cells drive antigen-specific latency reversal and immune elimination of persistent HIV-1. EBioMedicine 43:295-306.

10. Zaccard CR, Watkins SC, Kalinski P, Fecek RJ, Yates AL, Salter RD, Ayyavoo V, Rinaldo CR, Mailliard RB. 2015. CD40L induces functional tunneling nanotube networks exclusively in dendritic cells programmed by mediators of type 1 immunity. J Immunol 194:1047-56.

11. Puhr S, Lee J, Zvezdova E, Zhou YJ, Liu K. 2015. Dendritic cell development-History, advances, and open questions. Semin Immunol 27:388-96.

12. Steinman RM, Banchereau J. 2007. Taking dendritic cells into medicine. Nature 449:419-426.

13. Collin M, Bigley V. 2018. Human dendritic cell subsets: an update. Immunology 154:3-20.

14. Gardner A, de Mingo Pulido Á, Ruffell B. 2020. Dendritic Cells and Their Role in Immunotherapy. Front Immunol 11:924.

15. Nutt SL, Chopin M. 2020. Transcriptional Networks Driving Dendritic Cell Differentiation and Function. Immunity 52:942-956.

16. Hörig H, Medina FA, Conkright WA, Kaufman HL. 2000. Strategies for cancer therapy using carcinoembryonic antigen vaccines. Expert Rev Mol Med 2:1-24.

17. Jutel M, Akdis CA. 2011. T-cell subset regulation in atopy. Curr Allergy Asthma Rep 11:139-45.

18. Tang T, Cheng X, Truong B, Sun L, Yang X, Wang H. 2021. Molecular basis and therapeutic implications of CD40/CD40L immune checkpoint. Pharmacol Ther 219:107709.

19. Elgueta R, Benson MJ, de Vries VC, Wasiuk A, Guo Y, Noelle RJ. 2009. Molecular mechanism and function of CD40/CD40L engagement in the immune system. Immunol Rev 229:152-72.

20. Karnell JL, Rieder SA, Ettinger R, Kolbeck R. 2019. Targeting the CD40-CD40L pathway in autoimmune diseases: Humoral immunity and beyond. Advanced Drug Delivery Reviews 141:92-103.

21. Schoenberger SP, Toes REM, van der Voort EIH, Offringa R, Melief CJM. 1998. T-cell help for cytotoxic T lymphocytes is mediated by CD40–CD40L interactions. Nature 393:480-483.

22. Koch F, Stanzl U, Jennewein P, Janke K, Heufler C, Kämpgen E, Romani N, Schuler G. 1996. High level IL-12 production by murine dendritic cells: upregulation via MHC class II and CD40 molecules and downregulation by IL-4 and IL-10. J Exp Med 184:741-6.

23. Garcia-Bates TM, Palma ML, Shen C, Gambotto A, Macatangay BJC, Ferris RL, Rinaldo CR, Mailliard RB. 2019. Contrasting Roles of the PD-1 Signaling Pathway in Dendritic Cell-Mediated Induction and Regulation of HIV-1-Specific Effector T Cell Functions. J Virol 93.

24. Couch Y, Buzàs EI, Di Vizio D, Gho YS, Harrison P, Hill AF, Lötvall J, Raposo G, Stahl PD, Théry C, Witwer KW, Carter DRF. 2021. A brief history of nearly EV-erything - The rise and rise of extracellular vesicles. J Extracell Vesicles 10:e12144.

25. Raposo G, Nijman HW, Stoorvogel W, Liejendekker R, Harding CV, Melief CJ, Geuze HJ. 1996. B lymphocytes secrete antigen-presenting vesicles. J Exp Med 183:1161-72.

26. Gurunathan S, Kang MH, Jeyaraj M, Qasim M, Kim JH. 2019. Review of the Isolation, Characterization, Biological Function, and Multifarious Therapeutic Approaches of Exosomes. Cells 8.

27. Das Gupta A, Krawczynska N, Nelson ER. 2021. Extracellular Vesicles-The Next Frontier in Endocrinology. Endocrinology 162.

28. Doyle LM, Wang MZ. 2019. Overview of Extracellular Vesicles, Their Origin, Composition, Purpose, and Methods for Exosome Isolation and Analysis. Cells 8.

29. Kalluri R, LeBleu VS. 2020. The biology, function, and biomedical applications of exosomes. Science 367.

30. Sharma S, Rasool HI, Palanisamy V, Mathisen C, Schmidt M, Wong DT, Gimzewski JK. 2010. Structural-mechanical characterization of nanoparticle exosomes in human saliva, using correlative AFM, FESEM, and force spectroscopy. ACS Nano 4:1921-6.